Sustainable pollutant removal and wastewater remediation using TiO₂-based nanocomposites: A critical review

Md. Burhan Kabir Suhan [a], Md. Rashid Al-Mamun [b,c], Nawshin Farzana [a], Sirazam Munira Aishee [a], Md. Shahinoor Islam [a,d,*], Hadi M. Marwani [e,f], Md. Munjur Hasan [e,f,g], Abdullah M. Asiri [e,f], Mohammed M. Rahman [e,f], Aminul Islam [g,h], Md. Rabiul Awual [g,i,j,**]

[a] Department of Chemical Engineering, Bangladesh University of Engineering and Technology, Dhaka-1000, Bangladesh
[b] Department of Chemical Engineering, Jashore University of Science and Technology, Jashore 7408, Bangladesh
[c] Department of Civil and Environmental Engineering, University of Alberta, Edmonton T6G 1H9, Alberta, Canada
[d] Department of Textile Engineering, Daffodil International University, Dhaka 1341, Bangladesh
[e] Center of Excellence for Advanced Materials Research, King Abdulaziz University, Jeddah 21589, Saudi Arabia
[f] Chemistry Department, Faculty of Science, King Abdulaziz University, Jeddah 21589, Saudi Arabia
[g] Dhaka Institute for Materials Science (DIMS), University of Dhaka, Dhaka 1000, Bangladesh
[h] Department of Petroleum and Mining Engineering, Jashore University of Science and Technology, Jashore 7408, Bangladesh
[i] Materials Science and Research Center, Japan Atomic Energy Agency (JAEA), Hyogo 679-5148, Japan
[j] Western Australian School of Mines: Minerals, Energy and Chemical Engineering, Curtin University, GPO Box U 1987, Perth, WA 6845, Australia

ARTICLE INFO

ABSTRACT

Rapid industrialization and urbanization emphasized water purification and the production of carbon-neutral fuels. State-of-the-art technology that is low-cost, long-lasting, and easy to implement is required to address these issues. In this context, substantial developments in green synthesis technology have provided a more efficient, effective, and affordable procedure. One possible paradigm worth considering is a circular system that purifies water and produces biomass. Titanium dioxide-based photocatalysts (TPs) can be a great tool due to their outstanding properties, which can be modified for improving photocatalytic activities in various advanced oxidation process applications. In recent years, there has been a significant increase in the attention given to the development of environmentally sustainable TPs. A comprehensive analysis of nearly 300 academic articles in this study has revealed significant shortcomings in effectively utilizing TPs. The primary objective of this paper was to address these gaps that need to be filled in order to ensure the efficient and sustainable utilization of TPs in wastewater treatment. Accordingly, this paper comprehensively reviewed TiO₂'s features, including structure, properties, synthesis methods, photocatalytic activities, mechanism, structure modifications, applications, treatment cost analysis, and catalysts reuse in wastewater treatment. Finally, in order to ensure the sustainability of this wastewater treatment technique and achieve the goal of the circular economy, the concept of waste-to-resource has been introduced. The implementation of the aforementioned approach may serve as a valuable means of achieving environmentally sustainable outcomes in the field of wastewater treatment.

1. Introduction

Growing populations and economies have resulted in a dramatic increase in demand for water. Therefore, 36% of the global population lives in areas with inadequate water supplies. Contaminated water quality and insufficient water supply are only two of the many water-related difficulties posed by rapid urbanization, especially in low- and middle-income nations. There are monetary and economic advantages to maintaining water supplies, such as energy, reusable water, biosolids, and nutrients recovered from wastewater facilities. By applying circular economy principles to wastewater treatment, it may be possible to make sanitation self-sustaining and economically profitable through resource

recovery and reuse. Better wastewater management provides a dual value proposition if financial gains cover operating and maintenance costs [1–4].

With increasing industrial activities of civilization, many toxic chemicals are being released in wastewater. Complete removal of non-biodegradable pollutants is challenging to achieve by existing biological treatment processes [2,5–9]. Advanced Oxidation Process (AOP) involves the application of free hydroxyl radicals to oxidize the organic contaminants of the effluent [10–14]. The rapid and non-selective oxidation of organic matter in water is facilitated by photocatalysis, an AOP. In heterogeneous photocatalysis, a semiconductor catalyst speeds up the photoinduced process. Suspending the photocatalyst in solution and irradiating it with light is one of the simplest uses of photocatalysis [15–18].

Akira Fujishima and Kenichi Honda first reported the photocatalytic activity of nano TiO_2 in 1972 [19]. However, its application to environmental remediation started in the 1980 s after Frank and Bard removed cyanide ions from an aqueous solution through TiO_2 powder [20]. Since then, researchers are trying to explore effective methods of utilizing TiO_2 in effluent treatment [21]. The most effective use of AOPs is the combination of TiO_2 and ultraviolet (UV) light. The use of solar irradiation has the potential to improve the process energy efficiency and cost-effectiveness significantly. Researchers have done several investigations to create a visible light-active TiO_2 photocatalyst. In order to be activated, the TiO_2 photocatalyst must be exposed to UV visible (UV–vis) light. The use of a floating catalyst may achieve proper use of solar irradiation. In order to maximize their exposure to UV light, these catalysts are designed to float on the water's surface [22–24]. Wang et al. detailed various approaches to synthesizing TiO_2, including the sol-gel, solvothermal, and reverse micelle methods. In addition, the processes of TiO_2 synthesis have been published, along with the benefits and drawbacks of the techniques used and the environmental applications of photocatalytic products [25,26].

However, TiO_2 has certain limitations that prevent it from being widely used in photocatalysis. TiO_2's non-porous, polar surface, limited absorption capacity for non-polar organic pollutants, and aggregation and agglomeration of catalysts are only a few of the challenges it faces in the field of photocatalysis. Others include the coexistence of electrons and holes in the particle and their greater recombination probability, slower rates of the desired chemical changes in relation to the absorbing light energy, and a relatively large band gap energy (3.2 eV) [27–31]. Numerous studies on TiO_2 modification to improve its photocatalytic capabilities have been reported. These alterations have been made in various ways, such as doping with metals and non-metals, dye sensitization, surface modification, synthesis of composites with other materials, and immobilization and stabilization of support structures. Modified TiO_2 always has different qualities from pure TiO_2 in terms of how well it absorbs light, how well it separates charges, how well it adsorbs organic pollutants, how well it stabilizes the TiO_2 particles, and how easily it can be separated into individual TiO_2 particles [10,32–34]. Improving the photolytic activity by modifying the structure of TiO_2 for the photodegradation of wastewater pollutants has the potential to be an economically viable process, especially for large-scale plants.

Almost every type of industrial wastewater can be treated with the TiO_2 process. This includes textile wastewater [11,30,35–37], municipal wastewater [38,39], coffee-producing wastewater [40], pharmaceutical wastewater [41–43], petroleum processing wastewater [44,45], pesticides industry wastewater [46,47], paper mill wastewater [48–50], olive mill wastewater [51,52] and hospital wastewater [53].

The capacity to recycle a photocatalyst is crucial for keeping production costs down, but this problem has not been extensively investigated. The decreased efficiency of photocatalytic activity during reuse may have been caused by the loss of photocatalytic particles to the water or/and the buildup of intermediates with a poisonous impact on the surface of the nanoparticles. Ecofriendly, cost-effective, and reusable approaches to the treatment of polluted water approaches have the

potential to be ideal for expanding green photocatalyst systems [24,54, 55].

Lastly, in the nanostructured TiO_2 catalysts, where many studies have been conducted, there are notable knowledge gaps, particularly in efficiently producing these catalysts, their effectiveness in wastewater treatment, and their sustainable reuse. Our study addresses these existing voids and introduces innovative concepts, such as recycling these catalysts and exploring diverse TiO_2-based treatment methods for wastewater, focusing on their sustainability and environmental impact. Furthermore, we delve into the intriguing realm of CO_2 utilization, exploring how nanostructured TiO_2 can play a pivotal role in mitigating ecological challenges while progressing toward the ultimate goal of a circular economy. By shedding light on these innovative aspects, our research offers a comprehensive overview of recent advancements and presents promising pathways for leveraging nanostructured TiO_2 in environmentally responsible applications.

2. Structure and properties of TiO_2

TiO_2 is highly significant in theoretical and experimental studies due to its intriguing electrical structures and wide bandgap (3.2 eV for anatase). As a pigment, photocatalyst, and UV absorber, it has a wide variety of industrial Since fuel cells and solar cells require TiO_2, as well as pollution control and waste management systems and self-cleaning glass coating materials as well as food, cosmetics, paint, UV protection and many other uses for TiO_2, it is toxicologically inert, chemically stable, poorly soluble, and having a high refractive index. TiO_2 crystals have three primary crystal structures (Fig. 1A): anatase (which is stable at low temperatures, tetrahedral crystal structure), brookite (which is often found in minerals with an orthorhombic crystal structure), and rutile (which is stable at a higher temperature, tetrahedral crystal structure). Tetragonal crystals of anatase and rutile are produced from titanium octahedron (TiO_6), which has six oxygen atoms on each side of the six titanium atoms. The distortion and connection between the octahedrally coordinated Ti and O atoms differ only in configuration. At a lower synthesis temperature (600 °C), TiO_2 nanoparticle tends to nucleate to an anatase phase as surface Gibbs free energy is lower for the anatase phase than the rutile [56–58].

The surface is critical in solid-state materials because different surfaces may have significantly different characteristics. A material's surface greatly influences its physical and chemical properties at the nanoscale. Scientists have concentrated on improving the material's properties by altering the surface structure [56,59]. The agglomerated microstructure, porosity, and particle size of the material also influence the physical properties of TiO_2. In addition, there are several physical and chemical processes in which molecules on the surface of a particle are more active than those within, including charge transfer and chemical reaction. As a result, the character of TiO_2 nanoparticles with a larger surface-to-volume ratio gives greater efficiency.

In order to fully explore TiO_2 potential for applications, capturing light over the visible spectrum is critical, as is adjusting the basic optical bandgap of existing phases. To do so, a thorough understanding of its electrical and optical characteristics is required experimentally and theoretically. However, theoretical study relating to the compilation of TiO_2 polymorphs is limited. In an academic study, density functional theory (DFT) offers a basic framework for quantum many-body problems. It contributes considerably to creating novel materials and tuning and analyzing many material characteristics at the theoretical level. The functional choice affects the crystal structure of rutile, anatase, and brookite TiO_2. It's vital to utilize the proper exchange-correlation functional in density functional theory (DFT) calculations to acquire accurate results that match actual experimental findings and to provide reliable forecasts for new materials. In the study of Mohamad et al., when using the local density approximation (LDA), the band gap predicted by DFT for rutile TiO_2 was about 2.0 eV, which was around 33% lower than what was found experimentally. Due to inherent weak spots
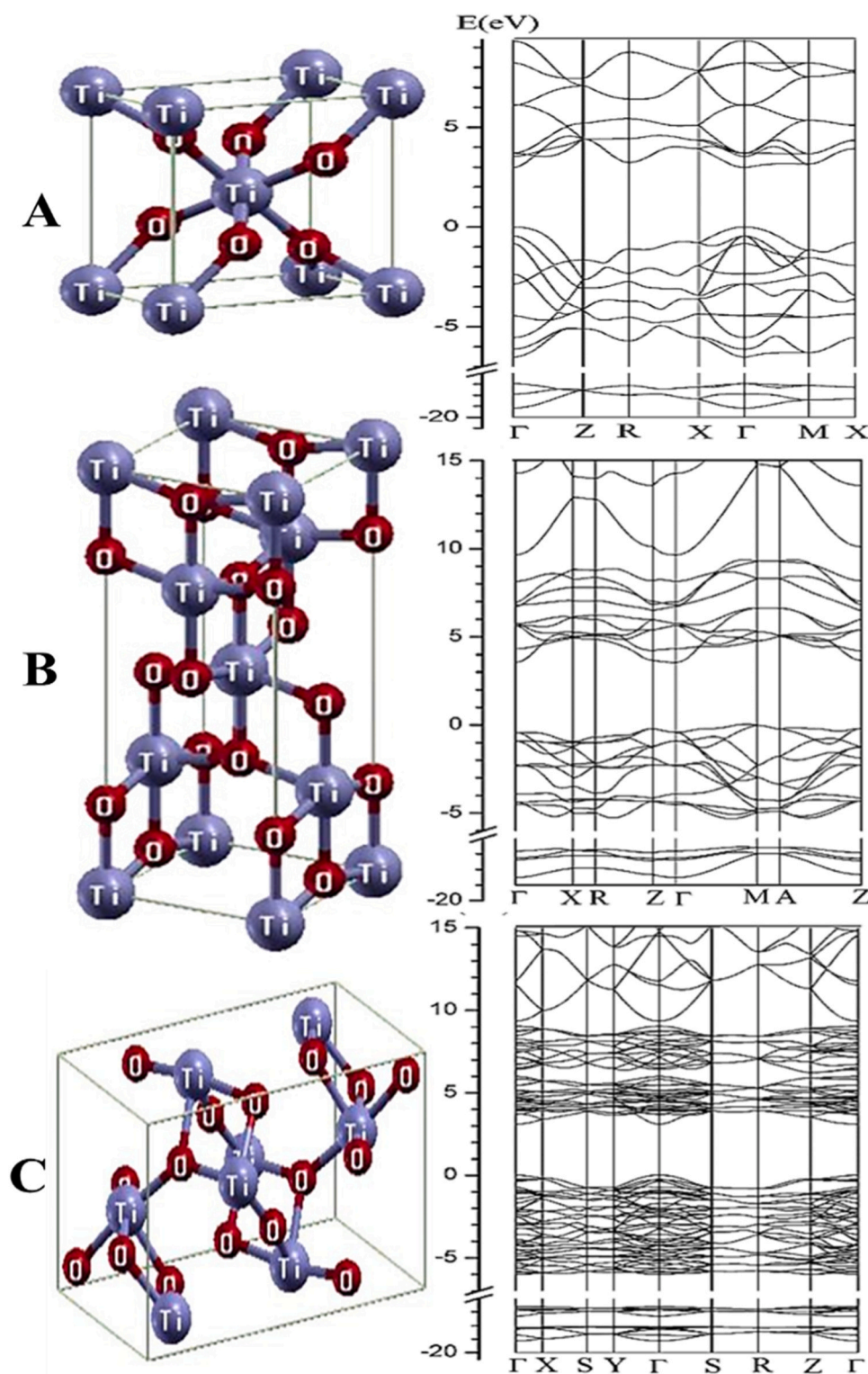
Fig. 1. Crystal and band structures of A) rutile, B) anatase, and C) brookite TiO$_2$. The valence-band maximum was taken as the energy zero [214,279].

associated with the Hartree-Fock (HF) approximation, this also differs from HF theory in that the experimental band gap is three times larger than the theoretical one. In the study of Zhang et al., rutile, anatase, and brookite TiO$_2$ band structures were studied. They found that the electronic structure and the polarized reflection spectra of brookite were similar to that of the rutile or anatase phase (Fig. 1B). Moreover, when it comes to optical properties and the process of photocatalysis, determining an adequate band gap for TiO$_2$ using a theoretical method is vital. Improved forecasts of the bulk band gap will definite the characteristics of the TiO$_2$ surface properties. Table 1 summarizes the structural, electronic, and optical properties of TiO$_2$ found experimentally and theoretically.

Table 1
Structural, electronic and optical properties of TiO$_2$ found experimentally and theoretically [211–214].

Structure	Position		Lattice parameters		Static dielectric value, $\varepsilon_{1\,(0)}$		Refractive index value, n$_{(0)}$		Band gap value	
	Ti	O	Method	a,b,c	PBE-GGA	mBJ-GGA	PBE-GGA	MBj-GGA	Experimental	MBj-GGA
Rutile	(0,0,0); (½,½,½)	O$_1$: $\pm$ (u,u,0); $\pm$ (u+½, ½-u, ½)	Experimental	a: 4.59;c: 2.96	7.98841	5.94684	2.82641	2.43863	3.00	2.71
			PW-LDA	a: 4.55;c: 2.92						
			PBE-GGA	a: 4.63;c: 2.98						
Anatase	(0,0,0); (0, ½, ¼); (½,½,½); (½,0, ¾)	O$_1$: (½,0,u-¼); (0,½, ¼-u); (½,½,½-u); (0,0,u); (0,½,¼+u); (½,0,¾-u); (0,0,ū); (½,½,½+u)	Experimental	a: 3.79;c: 9.51	5.82108	4.64421	2.41271	2.15506	3.21	3.02
			PW-LDA	a: 3.76;c: 9.47						
			PBE-GGA	a: 3.81;c: 9.63						
Brookite	(0.129, 0.104, 0.138)	O$_1$: (0.006, 0.093,−0.199); O$_2$: (0.237,0.161,0.461);	Experimental	a:9.18;b: 5.45;c: 5.15	6.26364	4.90509	2.50275	2.21476	3.13	3.14
			PW-LDA	a: 9.13;b: 5.41;c: 5.09						
			PBE-GGA	a: 9.26;b: 5.51;c: 5.17						

2.1. TiO$_2$ nanoparticle synthesis

The semiconductor materials are a vital part of photocatalysis primarily dependent on the synthesis technique. The nano-sized TiO$_2$ particles are preferred in AOPs compared with large particles due to their enhancement of molecular transport properties at the catalyst surface [60]. The two most essential characteristics of NPs have been introduced that make them preferable to the macroscopic or microscopic for textile effluent treatments are (i) the quantum bonds in nano-scale, which is accomplished through the holes and electrons sites, and (ii) surface and volume proportion which confirms the reaction improvement because of their considerable interaction through the functional sites [61]. However, nano-sized TiO$_2$ semiconductor is considered the most superior photocatalyst, which has been prepared in various shapes and sizes that include nanorods, nano bowls, nanospheres, nanofilms, nanoparticles, nanodisks, nanotubes, nanoneedles, nanosheets, nanowires, nanowhiskers, etc. [62,63]. Several synthesis routes, namely sol-gel, chemical precipitation and vapor, pyrolysis, electrochemical deposition, hydrothermal, etc., have been applied to prepare nano-size TiO$_2$ that gives certain benefits based on properties [64–66]. The synthesis technique varies with their reaction parameters such as precursors, solvents, contact time, pH, atmospheric condition, reaction temperature, degree of calcination, stirring speed, etc., which results in the change of morphological and optoelectronic properties of NPs [67,68]. Additionally, each technique possesses various operating conditions with unique advantages/disadvantages and varies from one method to another, as shown in Table 2. Based on the literature, it is easy to control the shape and size of prepared NPs by modifying these methods [67].

3. Mechanism of TiO$_2$'s photocatalytic degradation

TiO$_2$-based treatment is considered an efficient heterogeneous photocatalytic method as it uses energy from light to break down different organic and inorganic compounds in wastewater [69]. There are five steps to be considered for the photocatalytic degradation of pollutants by TiO$_2$:

First, i) a considerable amount of organic pollutants is carried from a solution into the interface area, where ii) they are adsorbed on the photon-activated TiO$_2$ surface, iii) photocatalyzed, and then iv)

desorption of degraded organic contaminants happens on the TiO$_2$ surface. After that, v) degraded organic contaminants (intermediate/ mineralized products) are removed from the interface region. The slowest step influences the overall pace of the reactions during organic pollutant degradation. The mass transfer steps (i) and (v) are very fast when compared to the reaction steps (ii), (iii), and (iv). As a result, steps (i) and (v) are not considered rate limiting and do not affect the total rate of photocatalytic processes. The process involves the production of the hydroxyl radical (●OH, oxidation potential = 2.8 V, relative oxidation power = 2.06), a powerful oxidizing agent employed to remove hazardous pollutants adsorbing on the TiO$_2$ surface [70,71].

Previously, rutile (bandgap 3.0 eV) and anatase (bandgap 3.2 eV) phases of TiO$_2$ semiconductors in the presence of light are extensively studied. Fig. 2 illustrates the primary mechanism of photocatalytic degradation of organic pollutants under the Solar-TiO$_2$ process based on the previous study findings. According to them, under solar light irradiation (photons), electrons and positive holes are generated in the conduction (e_{cb}^-) and valence band (h_{vb}^+) as explained in Eq. 1. The holes can either react with H$_2$O (Eqn. 2) or OH$^-$ (Eq. 3) organic molecules to generate hydroxyl radical or directly react with organic pollutants (Eqn. 10) that subsequently oxidize organic molecules. The breakdown of organic molecules is mainly caused by this ●OH radical (Eqn. 9). However, the electrons generated from the Eq. 1 can also participate in the breakdown of organic compounds indirectly either by producing superoxide anion radical (O$_2^{\bullet-}$) (Eq. 4), hydroperoxy radical (●HO$_2$) (Eq. 5), hydroxyl (●OH) (Eq. 7) or directly react with organic compounds to provide reduction products (Eqn. 11). In addition, the superoxide anion radical prevents the recombination of electron-hole pairs. Therefore, limited oxygen presence in the wastewater reduces the generation of O$_2^{\bullet-}$, enhances the recombination of electron-hole pair of TiO$_2$, and further reduces the catalytic activity of TiO$_2$ catalysts. The other intermediate and final significant steps are presented in Eqs. 6, 8 [70,72,73].

$$TiO_2 + h\nu \rightarrow TiO_2\left(h_{VB}^+ + e_{CB}^-\right) \tag{1}$$

$$TiO_2\left(h_{VB}^+\right) + H_2O \rightarrow TiO_2 + H^+ + OH^\bullet \tag{2}$$

$$TiO_2\left(h_{VB}^+\right) + OH^- \rightarrow TiO_2 + OH^\bullet \tag{3}$$

$$TiO_2\left(e_{CB}^-\right) + O_2 \rightarrow TiO_2 + O_2^- \tag{4}$$

5

Table 2
Features of different nanoparticle synthesis techniques.

Method	Photocatalyst	Precursor	Solvent	pH	Reaction time, (h)	Stirring type	Drying temperature, (°C)	Annealing temperature, (°C)	Annealing time, (h)	Advantages	Disadvantages	Reference
Sol-gel method	TiO_2 NPs	Titanium tetra-iso-propoxide	Isopropanol	—	3.0	Vigorous stirring	100 °C for 6 h.	500	3.0	-Low cost, low temperature, and easy maintenance in the laboratory. -Control over chemical composition, volume, and morphology. -Required a small quantity of dopant and good mixing capability. -Enhanced homogeneity, reliability, and purity than raw materials. -High purity and desired stoichiometry. -Ability to produce high-quality crystals.	-High fabrication cost. -long reaction time. -High temperature calcination. -Require organic solvents.	[215, 216]
Hydrothermal method	TiO_2 NPs	Titanium tetrachloride	Ethanol	7.0	0.5	Continuous stirring	50 °C for overnight	100–500	—	-Control over size-selective growth, and morphology -Simple and elegant mode of operation. -Low energy consumption -Capable of multi-layer fabrication. -Low temperature required.	-High temperature required. -High cost of autoclaves. -Longer reaction time.	[216, 217]
Spray pyrolysis method	TiO_2 microspheres	Titanium (IV) isopropoxide	Anhydrous ethanol	—	1.0	Vigorous stirring	—	500	1.0	-Different precursors are needed. -Homogeneity, control stoichiometry, and operate at atmospheric pressure. -Good adhesion and compatibility. -Capable of multi-layer fabrication. -formulates. -Excellent morphology with texture capability. -Uniform coating thickness.	-No uniform coating thickness.	[218, 219]
Chemical vapor deposition method	TiO_2 spheres	Titanium (IV) butoxide	Absolute ethanol	3–10	1.0	Continuous stirring	80 °C for 3 h.	450	1.0	-Comparatively cheap and simple. -Control homogeneity such as shape and size. -Good chemical stability and lower conductivity. -Higher quality coatings.	-High cost. -Required safety due to contamination. -Reaction temperature higher. -Deposition rate is lower.	[220, 221]
Electrochemical deposition method	TiO_2-Co composite	Titanium tetra isopropoxide, Cobalt (II) nitrate	Absolute ethanol	—	0.5	Vigorous stirring	50 °C for 24 h.	500	2.0	-Control over deposition rates. -Highly sensitive	-Costly and high flammability. -High electrical field strength is needed. -Toxicity and volatility.	[64,222]
Thermal plasma method	TiO_2 NPs	Titanium trichloride	Water, Sodium chloride	—	12.0	Continuous stirring	60 °C for 12 h.	300	2.0	-Highly sensitive	-Produce toxic byproducts. -Contaminate	[223, 224]

Table 2 (*continued*)

Method	Photocatalyst	Precursor	Solvent	pH	Reaction time, (h)	Stirring type	Drying temperature, (°C)	Annealing temperature, (°C)	Annealing time, (h)	Advantages	Disadvantages	Reference
Sputtering deposition method	TiO$_2$-Ag NPs	Titanium tetra isopropoxide, Silver nitrate	Isopropanol	—	0.5	Continuous stirring	100 °C for 2 h.	500	2.0	temperature. -Required lower temperature. -Excellent uniformity, porosity, and good adhesion capacity. -Lower temperature operation. -Uniform, high quality, and easy to control sputtering speed easily. -Good adhesion capability. -It is convenient and provides large area coatings. -Relatively simple and effective method.	chemicals and particles. -Equipment cost is higher. -Plasma contamination or damage. -Possible grainy and porous films. -Scarcity of substrate damage due to ionic bombardment.	[61,225]
Chemical precipitation method	TiO$_2$ NPs	Titanium (IV) oxalate solution	Oxalic acid, Deionized water	7.0	1.0	Vigorous stirring	100 °C for 5 h.	450	2.0	-Environmentally friendly. -Implementation and monitoring process is easy. -Low-temperature method and can be easily scaled up.	-Expensive process for treatment. -Poor crystallinity. -Requires basic condition. -Not applicable for all cases.	[224, 226]
Micro-emulsion method	TiO$_2$-Co-Fe Composite	Titanium isopropoxide	Acetyl acetone, L-threonine	—	1.0	Constant stirring	25 °C for 48 h.	500	3.0	-Thermodynamically stable -Excellent solvent action. -Temperature-sensitive and only remain stable in a specific temperature stability range.	-Environmental parameter effect on stability. -Stabilization requires a high amount of surfactants. -Limited solubilizing capacity for high-melting Substances. -Time-consuming and expensive for a relatively thick layer.	[227, 228]
Electro-deposition method	TiO$_2$-CdSe Composite	Titanium foils, Cadmium chloride, Selenium dioxide	Ethyl alcohol	2.0	0.5	Continuous stirring	Dried in air	500	2.0	-Enhanced the adhesion on the substrate -Able to dope. -Cost-effective	-Have limitations on the size and strength of electrodeposition. -Continuous process layout is more difficult. -Sometimes the material causes cracks and crevices in a built-up cavity.	[229, 230]
Microwave-assisted	TiO$_2$ NPs	Titanium (IV) chloride	Ethanol, Acetone	—	1.15	Vigorous stirring	100 °C for 1 h	200	1.0	-Controlled over temperature and pressure.	-Require high temperature. -High cost in	[227, 231]

Table 2 (*continued*)

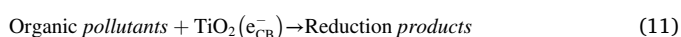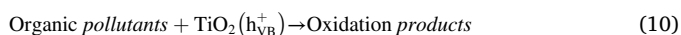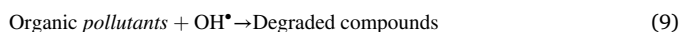| Method	Photocatalyst	Precursor	Solvent	pH	Reaction time, (h)	Stirring type	Drying temperature, (°C)	Annealing temperature, (°C)	Annealing time, (h)	Advantages	Disadvantages	Reference
hydrothermal method										-Reduce energy cost -Reaction time is short. -Efficient energy and environmentally friendly.	instrumentation. -Fuels are needed.	
Solvothermal method	TiO$_2$ NPs	Titanium tetra isopropoxide	Anhydrous ethanol	4.0	1.0	Homogeneously stirring	90 °C for 12 h.	400–500	1.0	-Control over size, shape, and crystallinity. -Enhance the chemical activity of the reactant. -Heat and pressure are applied up to a critical point.	-Require high temperature. -Observation of the reaction is impossible. -Expensive process and organic solvent required.	[229, 232]
Sono-chemical method	TiO$_2$ NPs	Titanium isopropoxide	Isopropanol	—	0.5	Continuously stirring	100 °C for 5 h.	500	2.0	-Provide relatively small particle size particle. -Provide high yield and short reaction time with a controlled reaction condition. -Velocity rates are high. -Uniform and high-purity shapes formed. -Provide better surface area.	-Sometimes irradiation time is long.	[229, 233]
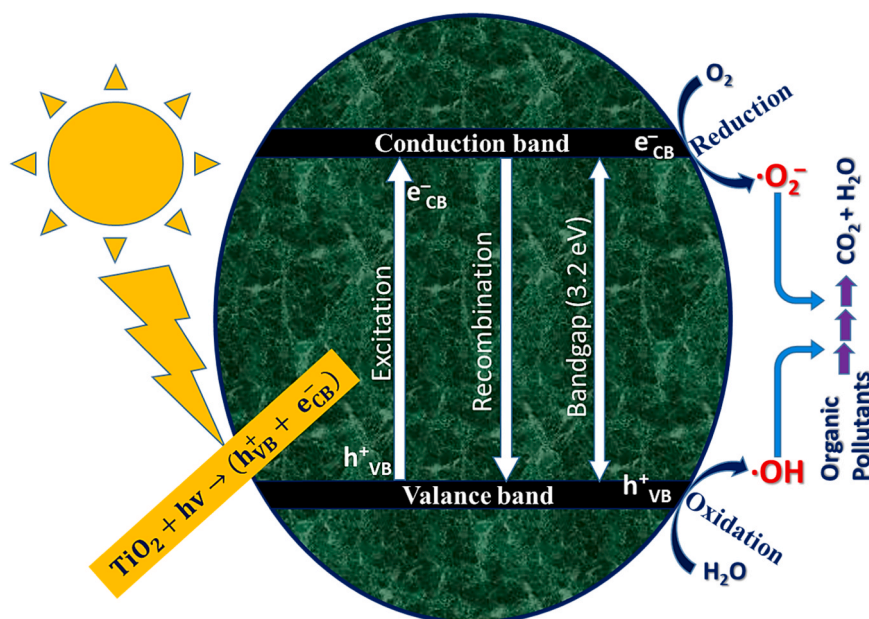
Fig. 2. Photocatalytic degradation of organic pollutants by TiO_2.

$$O_2^- + H^+ \rightarrow HO_2 \tag{5}$$

$$HO_2 + HO_2 \rightarrow H_2O_2 + O_2 \tag{6}$$

$$TiO_2\left(e_{CB}^-\right) + H_2O_2 \rightarrow OH^\bullet + OH^- \tag{7}$$

$$H_2O_2 + O_2^- \rightarrow OH^\bullet + OH^- + O_2 \tag{8}$$

$$Organic\ pollutants + OH^\bullet \rightarrow Degraded\ compounds \tag{9}$$

$$Organic\ pollutants + TiO_2\left(h_{VB}^+\right) \rightarrow Oxidation\ products \tag{10}$$

$$Organic\ pollutants + TiO_2\left(e_{CB}^-\right) \rightarrow Reduction\ products \tag{11}$$

Different dye molecules undergo unique reactions during the process of photocatalytic degradation, which involves the use of TiO_2 nanocatalysts and light. When Methylene Blue (MB) is subjected to UV or visible light, titanium dioxide produces electron-hole pairs. Electrons facilitate the reduction of oxygen, leading to the formation of superoxide radicals ($\bullet O_2$-). These radicals then engage in a reaction with MB, causing the disruption of its aromatic rings and culminating in the production of formaldehyde and smaller fragments. Conversely, holes undergo a reaction with water, generating hydroxyl radicals ($\bullet OH$) that further oxidize MB into CO_2 and water. In a similar way, the use of light-activated titanium dioxide induces the generation of electron-hole pairs in the presence of Rhodamine B (RhB). Specifically, the electrons originating from the aforementioned pairs engage in the reduction of oxygen, leading to the formation of superoxide and hydroxyl radicals. The conjugated system of RhB is susceptible to attack by these radicals, resulting in the degradation of the system into smaller pieces, which include CO_2 and organic acids. The breakage of azo bonds takes place in both Methyl Orange (MO) and Congo Red, leading to the formation of organic acids, carbon dioxide, and water in the case of MO, whereas Congo Red undergoes degradation into aromatic fragments, CO_2, and water [30,74–78].

4. Factors affecting the photocatalytic activity

Several factors influence the photocatalytic activity of the catalyst: extrinsic and intrinsic. Extrinsic factors are not a part of the reaction medium but influence its external towards the reaction. The extrinsic parameters are initial dye concentration, catalyst loading, light intensity, irradiation time, pH, and oxidant of effluent. Similarly, intrinsic factors influence its internal reaction and include crystal structure, particle size, shape, surface area, pore density, pore volume, and functional group of the catalyst [67,79].

4.1. Effect of dye amounts

The degradation and removal performance largely depend on the dye amount level. The most critical factor governing photocatalysis is the formation of $\bullet OH$ on the catalyst's surface and its interaction with the dye. It was observed that the increase in initial dye concentration decreased the photodegradation efficiency [80]. Generally, at higher dye concentrations, a large amount of dye molecules was adsorbed on the photocatalyst surface, which occupied the active sites as well as inhibited photon formation significantly and thus reduced the generation of $\bullet OH$ radicals [81]. Additionally, concentrated dye solution reduced the path length of a photon entering the solution, and suppressed the light passing to the catalyst, leading to a decrease in photocatalytic activity [82]. Illinous et al. has investigated the impact of various initial dye concentrations on the degradation of reactive yellow dye. It was found that the decreases in dye degradation efficiency (35.79–89.62%) with the increase of initial dye concentration from 25 to 100 mgL^{-1}. The reason might be the increase in dye concentration; the more dye molecules were found accessible for excitation and energy transfer [83]. Mamun et al. reported that the photodegradation efficiency of MO dye (45 mgL^{-1}) using a doped TiO2-based composite was decreased (23.0%) with the increase of initial dye concentration (50 mgL^{-1}) in the presence of solar light irradiation. This observation was formed due to inhibiting the penetration of simulated solar light into the dye solution [84].

4.2. Effect of catalyst loading

The degradation operation is influenced according to the quantity of TiO_2-based photocatalyst. The optimum loading must be determined to remove excess photocatalysts. The significant photocatalytic percentage is the ratio of the liquid amount to the pertinent photocatalyst. It can be seen that with the enhancement of catalyst dose, the functionality of the catalyst for high volume $\bullet OH$ radical is generation [85,86]. The degradation efficiency of reactive yellow 14 dye was increased from 52.6% to

91.3% using the photocatalyst loading (1–6 g/L) within 40 min. This was obtained due to some reasons, including (i) increasing the dye molecule's absorption area, (ii) increasing the density of particles in that area, and (iii) increasing the active sites of the area [87]. However, a large quantity of the catalyst that exceeds the optimal value may increase turbidity, decreasing the radiation rate of visible light and reducing the photodegradation efficiency [72]. Additionally, the higher catalyst particles tend to aggregate, decreasing the surface area, reducing the number of photons absorbed on the surface, and increasing light scattering, causing difficulty in UV/solar light penetration through the solution [80,86]. Caliskan et al. investigated the catalyst dose of zinc-doped TiO_2 composite from 0.5 to 1.5 g/L for the degradation of azo dye and found the optimum catalyst dose was 1.0 g/L under 3 h of UV irradiation [88].

4.3. Effect of irradiation time

The photodegradation efficiency has a proportional relationship with irradiation time. The photocatalytic reaction is increased up to a specific irradiation time, but evaporation starts when the temperature increases, resulting in inversely proportional to irradiation time. Thus, the photodegradation efficiency of organic pollutants was reduced with increased irradiation time [80]. This was formed due to producing more intermediate products, namely small chain aliphatic compounds that react with •OH and thus lead to a slower rate up to pertinent contact time. The TiO_2 film was prepared by dip-coating for the treatment of cationic Yellow X-Gl dye was studied. It was observed that the photodegradation efficiencies were 95.53%, 95.84%, and 99.14% for 1, 2, and 3 days, respectively, of UV irradiation [89].

4.4. Effect of light sources

The light source used for the degradation of the organic pollutants is essential as it determines the performance of the catalyst used. UV light intensity depends on the distance between the UV lamp and the photocatalyst, which controls the contaminant degradation efficiency of photocatalyst particles [90]. Recently, some reasons have been introduced for using UV irradiation sources for the degradation of textile wastewater, such as (i) power instability in long time operation, (ii) need for high voltage at initial stages, (iii) emitting border spectral wavelength, (iv) low photonic efficiency, (v) need available vapor pressure, (vi) shorter lifetime, and (vii) use of hazardous mercury metal [91]. Usually, a large volume of electron pairs was generated in the TiO_2 with the increase of intensity of light. These free radicals degrade the adsorbed contaminants on the photocatalyst surface [80]. The artificial UV light source is more reproducible and preferable than solar light exposure due to gaining more photodegradation efficiency in textile dyes. Thus, solar light irradiation is supposed to appear as an alternative cost-effective light source [92]. The degradation efficiency of acid orange 7 dye was observed to be almost 1.5 times higher in simulated solar light than in artificial UV light irradiation [93]. Literature reported that the degradation efficiency rose significantly to 56% with increased UV light intensity from 0 to 3.0 mW/cm^2. A similar trend was observed for the degradation of MO dye using TiO_2 NPs with power ranging between 17.25 and 65.85 W/m^2 and found efficiency (58.1–97.6%) after 180 min of UV irradiation [94]. However, a higher amount of light intensity did not contribute to higher degradation due to limited active sites of the TiO_2 NPs surface. Thus, optimum light intensity is required to obtain higher efficiency in photocatalytic reactions [72].

4.5. Effect of pH

The solution pH is one of the governing factors for the degradation of organics and the stability of the catalyst during photocatalysis. Typically, it depends on the point charge of the photocatalyst and the type of pollutant used in a reaction medium. The pH has always played a key role in pollutant remediation by diverse catalysts. It was reported that the oxidation kinetics increased with the increase in pH [95]. Several reports showed that dye adsorption was high in acidic pH regions [96]. Under acidic or basic regions, TiO_2 can be played as follows [86]:

$$TiOH + H^+ \leftrightarrow TiOH_2^+ \qquad (12)$$

$$TiOH + OH^- \leftrightarrow TiO^- + H_2O \qquad (13)$$

The value of pH_{pzc} of TiO_2 NPs is 6.8, varying from 4.5 to 7. It was reported that the TiO_2 surface will remain positively charged at an acidic medium (pH<6.8). This was formed because of its strong dye adsorption into the TiO_2 catalyst regarding electrostatic attraction. Similarly, a negative charge was obtained at a basic region (pH>6.8) because of the enhancement of TiO_2 groups into the TiO_2 catalyst. The higher oxidizing activity of TiO_2 NPs was found at low pH, but at very low pH, it generates a larger amount of H$^+$ ions that decrease the reaction rate. It influences the interaction between the catalyst surface and the solvent molecules during photocatalytic reactions. These observations greatly impact the adsorption of solutes, thus resulting in the photodegradation rate [85]. Based on the literature, the photodegradation of some organic pollutants using TiO_2 NPs is strongly favorable in an acidic medium compared to a basic or neutral medium. It was reported that the photodegradation efficiency of MO dye using TiO_2 NPs was increased in acidic pH (3.0) under 5 h of direct solar light irradiation [10]. Similarly, an anionic dye of acid orange 7 has shown a higher degradation efficiency at lower pH (3.0) [86]. For the photocatalytic degradation of reactive orange 4 dye, the decolorization was observed from 24.14% to 89.10% with the increase of pH from 1 to 10 at the reaction time of 80 min. Then, with a further pH increase from 10 to 12, the decolorization efficiency was obtained from 89.31% to 81.20% [97].

4.6. Effect of oxidant

Several oxidants such as H_2O_2, $S_2O_8^{2-}$, and BrO^{3-} are applied in photocatalysis, which greatly affects bio-persistent toxic dyes. The addition of an oxidant acts as a strong electron scavenger that increases the photodegradation efficiency of intermediate compounds through three different ways, including (i) suppressing the recombination of the electron-hole pair, (ii) generating a larger amount of •OH and $O_2^{•-}$ formation, and (iii) to increase charge separation. The dual nature of intermediate oxidants, such as strong oxidants and electron scavengers, is observed in photocatalytic reactions [60,96].

Generally, the peroxide is a supply of oxygen with high oxidant potential (E° = 1.77 V) that increases the reaction rate. The addition of H_2O_2 on photocatalysis for degrading organic dye compounds from textile wastewater was significant. The photo-oxidation rates have been increased by adding H_2O_2 since more •OH could be produced by reducing surface-trapped electrons. Therefore, the photodegradation performance might be uniformly increased with oxidative conversion by the addition of H_2O_2 [84]. As a result, •OH is generated by the reaction with conduction band electrons and hydroxide ions from water molecules. On the contrary, the mineralization rate is greatly influenced by the addition of $S_2O_8^{2-}$ oxidant by decreasing the pH of the dye solution [96]. Two different ways have been applied in reaction mechanisms such as (i) charge separation increases by scavenging persulphate ion, and (ii) sulfate radical anion ($SO_4^{•-}$) can be formed both in thermally and photolytically from $S_2O_8^{2-}$ in TiO_2 NPs suspension. The addition of BrO^{3-} plays an effective electron acceptor which enhances the photocatalytic rate as well as photodegradation efficiency of dye-containing textile wastewater [87]. This was formed because of the band electron and oxidant (BrO_3) interaction through the scavenging effect. However, the excess addition of BrO^{3-} reduced the photocatalytic activity of TiO_2 NPs under UV/solar light irradiation. The addition of $KBrO_3$ from 1 to 3 g/l for the degradation of reactive orange dye from textile wastewater increases the degradation efficiency from 64.4% to 97.97% within 20 min irradiation time [97].

4.7. Effect of particle size and surface area

The surface properties of a semiconductor are considered a major factor for enhancing photocatalytic activity and can be achieved by improving bandgap energy as well as photogenerated electron/hole recombination [60]. Additionally, the potential degradation rate is highly affected by the synthesized materials' surface properties, such as zeta potential, acidity, and isoelectric point [98]. Both nano and bulk-size TiO$_2$ surfaces have been evaluated extensively and observed significant variations in photodegradation performance and photochemical responses [99]. Several studies indicated that the smaller shapes create a more surface-to-volume ratio, and increase internal recombined electron/hole pairs and active sites of surface area, and therefore a large amount of •OH available to degrade organic pollutants [98]. The high surface area effectively enhanced the photogenerated charge carrier separation rate and provided charge transport efficiency [67]. Some drawbacks have been found when decreasing the particle size of TiO$_2$ photocatalyst, including (i) decreasing surface recombination of electron/hole pairs and (ii) lowering the utilization of photons. Therefore, an optimum particle size should be selected to overcome these challenges. It can be seen that the optimum particle size of the TiO$_2$ photocatalyst was 35 nm for the degradation of methylene blue dye under UV irradiation [72]. Bisphenol A (11.2 mgL^{-1}) was observed to be degraded at 96%, and 84% for nano and micro-structured TiO$_2$ film, respectively, within 2 h of UV irradiation [100].

4.8. Effect of surface morphology

It is well known that the photocatalytic activity of TiO$_2$ NPs is highly affected by surface morphological factors, including phase composition, crystallinity, crystal structure, porosity, pore volume, and surface hydroxyl groups [101]. Additionally, the preparation technique of the catalyst can significantly affect the surface morphology of NPs, such as precursor, solvent, pH, reaction time, and calcination temperature. Generally, the crystal structure of TiO$_2$ NPs depends on the calcination temperature. It was found that higher photodegradation performance was obtained by crystalline morphology than by amorphous morphology. The thermal treatment method has been applied to transform TiO$_2$ NPs from amorphous to crystalline phases [98]. Literature reported that the pure anatase phase with its adjacent lower rutile phase of TiO$_2$ NPs has shown greater photodegradation efficiency. The interface between the rutile and anatase phases may act as an electron trap due to their various Fermi levels [100].

5. Enhancing the performance of TiO$_2$

5.1. Doping

The development of new energy levels near the conduction band is increased by doping TiO$_2$ with different elements. A high concentration of the photocatalyst might diminish its effectiveness, therefore it's important to utilize just the right quantity for the best activity [102]. The type of the dopant ion also influences this activity since dopants might be interstitial, substitutional, or both in the case of incorporation. The characteristics of titanium dioxide vary depending on the doping region [103]. TiO$_2$ may undergo alterations either in the bulk or on the surface of TiO$_2$ particles to increase the absorbance of irradiation and decrease the charge recombination [24].

5.1.1. Metal doping

Recently, researchers have focused on improving photocatalysis activity by adopting a doping process with various compounds that can reduce undesirable [104]. The band gaps (3–3.2 eV) of TiO$_2$ semiconductors absorbing from the UV region of the solar spectrum are the major drawbacks in photocatalysis, as only about 5% of sunlight comprises UV radiation. Modifying the band gap in TiO$_2$ has become a

modern research interest that can be influenced either in bulk or on the surface of TiO$_2$. Doping metals or non-metals into bulk TiO$_2$ significantly affect bulk modifications. The doped catalysts displaying greater photo-stability in aqueous solution appear suitable for photocatalytic water remediation [105].

In the doping process, rapid charge recombination is inhibited, and the interfacial transfer of charge is enhanced by trapping holes or electrons in the defect sites in the first phase. Light absorbed was exhibited by allowing electron transitions under sub-band gap irradiation. The dopants are mainly categorized into metal ions (transition metals, noble metals, and rare earth metals) and non-metal ions. Metal dopants in the photocatalytic matrix significantly contribute to enhanced interfacial charge transfer and recombination rates, imparting improved photoactivity of doped TiO$_2$ [106]. As in Table 3, some metal dopants such as copper (Cu) [107], iron (Fe) [108], manganese (Mn) [109], nickel (Ni) [75], platinum (Pt) [110], zinc (Zn) [111], barium (Ba) [112] and cobalt (Co) [113,114] have been extensively utilized to reduce the band gap energy and to redshift the TiO$_2$ absorption from UV to leading to increased performances.

In a recent study by Juárez-Cortazar et al. (2022), metallic residue from door keys as a doping precursor was integrated with TiO$_2$ nanoparticles using the sol-gel route. Photoactivity was improved synergistically by the presence of Cu$^+$/Cu^{2+} and Zn^{2+} ions in the support modified the physicochemical characteristics of Titania. Mineralization of diclofenac was above 92% in an aqueous solution under simulated solar radiation. Some metal nanoparticles such as lead (Pd), silver (Ag), and Platinum (Pt) have been employed to expand the visible light sensitivity of the resultant TiO$_2$ hybrids (Table 3). Several techniques such as hydrothermal, electrospinning, chemical reduction, and UV radiation have been explored to prepare a cost-effective Ag/TiO$_2$ nano-hybrid photocatalyst which confirmed the restrictions of the recombination of electron-holes and enhanced the visible light absorption region [116,117].

5.1.2. Non-metal doping

It is observed from several studies over the last few years that the non-metal anion doping has been extensively applied to hinder the recombination of photogenerated electron-hole pairs which is attributed to the electronic states of non-metals above the valence band edge of nano-TiO$_2$. The non-metal doping is considered superior to metal doping because of provides higher stability of TiO$_2$ photocatalyst, a simpler doping process, and more photocatalytic activity. Different non-metal dopants such as nitrogen (N) [118], F-doped anatase TiO$_2$ [30], sulfur (S) [119], and carbon (C) [120] have been successfully explored in the modification of diverse catalysts.

Over 99% photodegradation of organic dyes within less than 2 h of UV exposure was achieved by N-TiO$_2$ and P-TiO$_2$ nanocatalysts prepared by microwave-assisted technique, respectively [121]. Another study by Azami et al. reported the complete degradation of reactive red 4 dye within 60 min under LED light by decreasing the band gap to 2.9 eV, introducing N dopants to TiO$_2$ through microwave irradiation [122].

Ordered N-TiO$_2$ nanotubes synthesized via an electrochemical approach degraded methylene blue by about 52% under xenon lamp irradiation for 120 min. It was stated that photocatalytic efficiency was improved by altering the TiO$_2$ band structure and reducing electron-hole charge recombination [123]. Doping S in TiO$_2$ through a novel flame spray pyrolysis method significantly reduced the bandgap energy (2.78 eV), stimulated the phase conversion of TiO$_2$, enhanced electrical conductivity and charge transfer leading to higher photocatalysis performance towards acetaldehyde upon visible light irradiation [119].

5.1.3. Metalloid and halogen doping

Various halogen dopants, including fluorine (F) [30], chlorine (Cl) [124], bromine (Br) [125], and iodine (I) [126], have been investigated so far for improving the structure and photocatalytic degradation of catalysts (Table 3). Boron (B) (Yu et al., 2013a) and silicon (He et al.,

Table 3

Summary of doping, co-oping, and coupling of TiO_2.

Nano photocatalyst	Preparation method	Target analyte	light source and treatment time	Removal efficiency	Reference
$Ba-TiO_2$	Sol-gel	Methylene blue	Solar light, 150 min	> 70%	[112]
$F-TiO_2$	Sol-gel	Methyl orange	UV light, 5 h	> 80%	[30]
$Zn-TiO_2$	Sol-gel	Methyl red	UV light, 2 h	96.99%	[111]
$Ni-N-TiO_2$	Sol-gel	Congo red and Methyl orange	Visible light, 2 h	82%, 79%	[75]
$Fe-TiO_2$	Ultrasonic assisted hydrothermal	Para-nitrophenol	Visible light, 5 h	92%	[108]
$Mn-TiO_2$	Sol-gel	Methylene blue	UV and Visible light, 5 h	…	[109]
$Pt-TiO_2$	Colloidal routes	Phenol, 2-chlorophenol	UV light, 3 h	87.7%, 100%	[110]
$Co-TiO_2$	Sol-gel	2-chlorophenol	UV light, 3 h	96.4%	[114]
$Ag-TiO_2$	Sol-gel	Methyl Orange	Visible light, 5 h	…	[234]
$F-WO_3-TiO_2$	Sol-gel	Methyl orange	UV light, 5 h	> 85%	[30]
$N-TiO_2$ nanotubes	Electrochemical method	Methyl blue	Xenon lamp, 120 min	52%	[123]
$N-TiO_2$	Sol-gel	Rhodamine B	Visible light, 40 min	90%	[235]
$N-TiO_2$	plasma-assisted electrolysis	Methyl orange	UV emitted by plasma, 300 min	91%	[236]
$S-TiO_2$	flame spray pyrolysis	acetaldehyde	visible light irradiation, 300 min	75%	[119]
$S-TiO_2$ nanorods	Oxidant peroxide method	Methyl blue	Visible light, 240 min	92%	[237]
$S-TiO_2$	Hydrothermal method	Rhodamine B	Visible light, 60 min	80%	[238]
Metallic residue-TiO_2	Sol-gel	diclofenac	Simulated solar light, 180 min	92%	[115]
$ZnO-TiO_2$	Sol-gel	Methyl blue	UV light, 6 h	…	[132]
$Cu-TiO_2-ZnO$	Sol-gel	Methyl blue, Methyl orange	Visible light, 3 h	83.35%, 75.5%	[239]
$Cu-TiO_2$ nanoparticles	Sol-gel and microwave hydrothermal	Diclofenac	Visible light, 7 h	33.26%	[107]
$N-Fe-Cu-TiO_2$ nanoparticles	Sol-gel	Methyl blue	Sunlight, 2 h	…	[78]
$N-Zr-TiO_2$ nanoparticles	Sol-gel	p-nitrophenol	UV–visible light, 8 h	96%	[78]
$Pt-Bi-TiO_2$	Modified photodeposition	AMX	Visible light,	87.67%	[128]
$Sn-La-TiO_2$	Sol-gel	Rhodamine B	UV light, 3 h	99.1%	[77]
$Er^{3+}:YAlO_3/Fe-Co-TiO_2-ZnO$	Sol-gel	azo fuchsine	Visible light, 2 h	95.5%	[240]
$TiO_2/Zr,N$ nanoparticles	Sol-gel	Waste water containing 2,4-dinitrotoluene (2,4-DNT); 2,6- dinitrotoluene (2,6-DNT) and trinitrotoluene (TNT)	Visible light, 12 h	67.2%	[130]
$Mn-Co-TiO_2$	Sol-gel	enoxacin	Solar light, 80 min	97%	[131]
$BaTiO_3-ZnO$	Hydrothermal method	Methyl blue	UV light, 60 min	94%	[133]
$Ti_3C_2/TiO_2/CuO$ ternary nanocomposites	Chemical reaction and annealing at Ar atmosphere	Methyl orange	UV light, 80 min	99%	[241]
$N-TiO_2/SiO2/Fe_3O_4$ Nanoparticles	hydrolysis and condensation, dispersion and calcination	phenol	Visible light, 270 min	64%	[134]
$Co_{0.5}Zn_{0.25}M_{0.25}Fe_2O_4-TiO_2$	Co-precipitation, hydrolysis, and thermal treatment	Methyl orange, Methyl blue	Visible light, 5 h	80%, 75%	[242]
Hematoporphyrin/$N-TiO_2$	Sol-gel and wet impregnation	Methyl orange	Visible light, 60 min	89.2%	[243]
Fe_3O_4/TiO_2-S with surface hydroxyls	one pot reverse precipitation and hydrothermal	Rhodamine B and formaldehyde	Simulated solar light, 60 min	100%	[244]
$TiO_2/zeolite$	Modified sol-gel	Reactive black 5	UV light, 120 min	100%	[245]
$TiO_2/zeolite$	Sol-gel	marbofloxacin and enrofloxacin	Natural sunlight, 2 h	91%	[246]

2010), termed either non-metal or metal, are the two most used metalloids used to dope TiO_2. Boron dopants have succeeded in increasing the surface area of embedded TiO_2.

5.1.4. Co-doping

Co-doping techniques have been proven to be affecting material properties. The OH^- of TiO_2 has been successfully increased by co-doping restraining. As in Table 3, explorations on significant co-doping techniques include $N-Fe-Cu-TiO_2$ nanoparticles [78], N/Zr co-doped TiO_2 nanoparticles [127], Pt and Bi Co-doped TiO_2 [128], Sn/La co-doped TiO_2 nanomaterials, S/I co-doped mesoporous TiO_2, Ce/N co-doped TiO_2 [129], WO_3 Coupled $PTiO_2$ etc. In addition, the researchers also reported that an optimal doping level was required for co-doping under visible light; otherwise, the photoactivity of TiO_2 may deteriorate.

Photocatalytic degradation of organic dyes was investigated under solar light irradiation with two photocatalysts. The results indicated that the $Er^{3+}:YAlO_3/Fe-$ and Co-doped TiO_2 coated composites significantly transform the visible light into the UV region and greater enhancement of the photocatalytic activities found by the addition of $Er^{3+}:YAlO_3$ as compared to Fe- and Co-doped TiO_2 powders.

In 2018, The photocatalytic performance of co-doped TiO_2/Zr, N nanoparticles in wastewater treatment of nitrotoluene samples containing 2,4-dinitrotoluene (2,4-DNT), 2,6- dinitrotoluene (2,6-DNT) and trinitrotoluene (TNT). The results showed 35.9–67.2% treatment efficiency and 3.17–2.78 eV band gap energies at different compositions of nanoparticles under visible light irradiation [130].

In another study, a novel Mn^{2+} and Co^{2+} co-doped TiO_2 (Mn-Co-TiO_2) was synthesized for the photocatalytic decomposition of enoxacin (ENX) in synthetic and real wastewater samples. Mn-Co-TiO_2 showed an ability to reduce the band gap of TiO_2 from 2.81 eV to 2.10 eV with improved morphological properties under solar light irradiation [131].

5.1.5. Coupling of TiO_2 with semiconductor

Various semiconductor catalysts such as MgO, SiO_2, CdS, WO_3, MoO_3, SnO_2, In_2O_3, Cu_2O, or ZnO [132] have been successfully coupled with TiO_2 by researchers to improve the characterizations, energy level, rigidity as well as to reduce band gap shifting the light absorption towards the visible region (Table 3). Another recent study was explored by

anchoring $BaTiO_3$ nanoparticles on the ZnO matrix by hydrothermal methods to produce a heterostructure, which confirmed UV-assisted photodegradation of methylene blue within 60 min. The heterojunction between $BaTiO_3$ and hexagonal rod-shaped ZnO promoted affected charge separation, contributing to about 94% removal of dyes [133]. Vaiano et al. introduced SiO_2/Fe_3O_4 ferromagnetic nanoparticles as support for N-doped TiO_2 to degrade phenol and eliminate TOC at 64% and 55%, respectively under visible light irradiation after 270 min. The magnetic photocatalyst displayed enough photostability after being collected at the bottom of the photoreactor after each test cycle (up to four recyclability tests) by employing a magnet on the outer surface of the reactor [134].

5.2. Plasma technology

Recently, photocatalytic treatments coupled with plasma technology have been a great research interest and have proven to be successful in the field of water pollutant reduction due to being the most efficient and environmentally safe [135]. The combining process leads to the efficient degradation of liquid-phase contaminants by enhancing photocatalytic reactions by the participation of higher active catalyst sites through the improved mass transports of the reactants to the solid surface which was basically due to the ultrasound and shockwave generation in the electrical discharge plasma.

Thermal plasma, such as arc discharges, radio frequency, or torches, is obtained with high electrical energy. In contrast, non-thermal plasma (NTP) is associated with less power consumption such as dielectric barrier discharge, corona discharge, gliding arc discharge, spark discharge, and glow discharge. In non-thermal plasma, the energetic electrons produce secondary electrons, photons, ions, and radicals through collision with background molecules (N_2, O_2, H_2O, etc.) [136].

These facts lead to the attraction for applications of atmospheric plasma treatment by gas electrical discharge systems in water remediation.

There are various types of non-thermal plasma photocatalytic rectors which can be categorized according to the type of power supply (DC, AC, AC and DC, pulse, DC and pulse, RF), geometry, discharge mode, polarity, electrode configuration, presence of a dielectric barrier or photocatalyst, input voltage/frequency level, and gas composition [137]. Table 4 depicts the summary of some Plasma/TiO_2 combined wastewater treatments. As in Table 4, Wang et al. integrated a pulsed corona discharge system with a TiO_2 powder photocatalyst to decompose phenol [138]. Similarly, the pulsed discharge system was coupled with TiO_2 film [139], TiO_2 powder [140], activated carbon fiber and TiO_2 powder hybrid catalyst [141], and TiO_2 nanoparticles [142] to degrade different organic substances from wastewater. Complete or maximum removal was only achieved with an integrated system (Table 4).

An interesting study was conducted by Pandiyaraj et al., 2021 to synthesize copper-doped TiO_2 nanoparticles by sol-gel technique. The prepared nanostructure was further subjected to plasma treatments (at 32 kV power supply) in a low-pressure DC glow discharge plasma reactor to enhance photocatalysis operated at various gas streams like in Ar, air, O_2, and N_2 at a fixed flow rate (9 lpm) for 10 min. The mechanism of photocatalytic activity was initiated through the emission of UV photons in the dye solution by plasma jet generating of electron-hole pair. This plasma-induced surface modification changed the oxidation state in Cu-TiO_2 nanoparticles, hampering the electron hole's recombination reaction by capturing the electrons and subsequently resulting in high photoactivity. The study also revealed that Ar plasma combined with N_2 plasma to treat nano-photocatalysts synergistically generated the highest concentration of reactive species such as $\bullet OH$ radicals and H_2O_2, exhibiting the highest photodegradation (94%) of reactive red 198. It was concluded that plasma-functionalized Cu-TiO_2

Table 4
Summary of Plasma/TiO2 combined wastewater treatments.

Type of photocatalyst	Plasma properties	Target analyte	Processing condition	Removal efficiency		Reference
				without photocatalyst	with photocatalyst	
Defect-rich Ar-TiO_2 nanoparticles	DBD	Methyl orange, rhodamine B and Methylene blue (10 mg/L)	50 V, Ar supply for 20 min, treatment time 30 min	-	99.4%	[247]
TiO_2-graphene nanocomposite	PDP	Fluoroquinolone (40 mg/L)	18 kV, air supply (4 L/min), treatment time:60 min	99.4%	64.8%	[248]
$AgFeO_2$/CNTs/TiO_2	Corona-DBD combined	Methyl Orange (250 ml, 30 ppm)	5 kv, air supply: 1 L/min, treatment time: 2 min	-	95%	[249]
TiO_2 nanoparticles	Needle plate	Reactive Orange 16	Argon with 10% air (4 slm), treatment time: 60 min	-	100%	[250]
TiO_2 nanopowders	Corona discharge	Tetracycline (50 mg/L)	36 W, air supply: 0.006 m^3/h, treatment time: 24 min	61.9%	85.1%	[144]
TiO_2-ACFs	DBD	Triclocarban (10 mg/L)	38 W, Dry air, oxygen, nitrogen and argon (400 ml/min) supply, treatment time:30 min	32%	64%	[251]
TiO_2-rGO nanocomposite	DBD	Acetaminophen (20 mg/L)	18 kV, pH: 7.2, air supply (3.3 L/min), treatment time: 18 min	50%	92%	[252]
Fe_2O_3-TiO_2 with $Na_2S_2O_8$	DBD	Dimethyl phthalate (100 mg/L)	14 kV, pH:3, air supply 0.5 L/min), argon supply (4.5 L/min)	100% (24.6 min)	100% (5.2 min)	[253]
g-C_3N_4/TiO_2	DBD	Acid Orange 7 (5 mg/L)	20 W, pH:10, air supply (0.014 L/min), treatment time 12 min	61%	100%	[223]
ACF/TiO_2	PDP	Methyl Orange (80 mg/L)	46 kV, pH:4, oxygen supply, treatment time 15 min	63%	98.2%	[141]
TiO_2 nanoparticles	DBD	Reactive Yellow 176 (200 mg/L)	70 W, pH:6.8, atmospheric air supply, 180 min	66.21%	83.54%	[254]
TiO_2 nanoparticles	PDP	Acid Orange 7 (600 ml)	27 kV, oxygen supply (1.4 m3/h), treatment time 45 min	81%	96%	[142]
TiO_2 supported beads	PDP	Phenol (0.25 L)	21 kV, oxygen supply (5 L/min), treatment time 40 min	60%	91.40%	[138]
TiO_2 film	PDP	Phenol (0.25 L)	24 kV, oxygen supply (1.33 L/min), treatment time 60 min	53%	78%	[255]
TiO_2 powder	PDP	4 Chlorophenol (0.1 L)	14 kV, oxygen supply (1.66 L/min), treatment time 18 min	74%	90%	[140]
TiO_2 nanofilm	PDP	Indigo Carmine	30 kV, air supply (0.5 m3/h), treatment time 3 min	86%	96%	[256]

nanostructures could be very promising for textile and pharmaceutical industries to abate organic pollutants [143]. From Table 4, another paper was reported to remove tetracycline (TC) and TOC from an aqueous solution by TiO_2 nanoparticles coupled with non-thermal plasma in a corona discharge plasma reactor with a high-frequency high voltage power source and a gas delivery system [144]. It was demonstrated that an increased amount of TiO_2 concentration contributed to about 85% removal efficiency of TC within 24 min at the input power of 36 W.

5.3. Coupling of TiO_2 with clay

Clay minerals, being hydrous aluminosilicates, retain large amounts of water, including some other important properties like colloidal behavior, adsorption capacities, and swelling as well and exist in their basic four forms viz., kaolinite, illite, montmorillonite (smectite), and chlorite [145]. Based on the academic context, clay is composed of fine-grained crystal minerals such as carbonates and other metal and non-metal oxides. The polytypic and structural arrangements in clay, called polytypism, account for different structural layers and compositions. These structures are commonly used due to their high surface area, stability, naturally abundant, non-toxicity, and significant roles in scavenging pollutants from wastewater. The nanocomposites of clay with TiO_2 had been successfully proven to possess higher photolytic activity with greater surface area, a higher degree of crystallinity, and regeneration possibilities for the degradation of contaminants from wastewater.

Nanocomposites like clay/TiO_2 are now attracting the attention of researchers due to their unique flexibility and improved properties such as greater affinity to the pollutants, enhancing antimicrobial solid properties, and hindering the release of nanoparticles [146]. Impediments to the large-scale use of TiO_2 in water remediation are its high band gap, fast electron-hole pair recombination, particle aggregation, and recycling after treatments. Immobilization of TiO_2 nanoparticles onto clays (phyllosilicates) can eliminate those by forming the Ti-O-Si and Al-O-Ti bonds between TiO_2 nanoparticles and the aluminosilicate layers of the clay support [147].

Clay materials such as montmorillonite (mt), kaolinite (kt), rectorite (rec), bentonite (bt), hectorite (hec), sepiolite (sep), Palygorskite (pal), Vermiculite (vem), laponite (lap), saponite (sap), cloisite (clo) have been studied most due to being stable, available and possessing good structural properties to act as supports with TiO_2 nanoparticles contributing to a high degree of photodegradation and scavenging contaminants from wastewater [146].

A simple adsorb-degrade-release mechanism in photocatalysis of TiO_2/Clay nanocomposites involves the adsorption of large molecules of contaminants on the clay support and active sites and degradation by the reactive oxygen species and release. High porosity and larger surface area allow fast conversion and mineralization of the degraded pollutants within the porous framework of the nanostructure and also a large quantity of pollutant molecules is thus allowed to come into contact with the active sites undergoing a higher degree of photocatalytic oxidation by the light exposure on more areas [147].

There are different methods involved in synthesizing binary, ternary, and quaternary TiO_2/clay nano photocatalysts. The binary TiO_2/clay photocatalysts are generally fabricated either by the simple dry diffusion (grinding) method [148] or the wet chemical (pillaring) process [149]. Single or multistep processes incorporated with the binary TiO_2/Clay structures to improve specific properties such as their visible region, surface area, and porosity for enhanced photocatalysis to synthesize ternary and quaternary nano-composites [147].

In another study, a novel TiO_2 intercalated montmorillonite (a cationic, dioctahedral smectite clay, [150]) photocatalyst was prepared by varying pH conditions to the conventional hydrothermal process

which allowed more active sites to the Ti^{3+} and larger pore volume thus promoting better photodegradation efficiency and stable recyclability to methyl orange dye degradation [151].

5.4. Carbonaceous and Bio-nanocomposites of TiO_2

This part focuses on the recent studies of some bio-based nanocomposites of TiO_2 for purifying water, which have been proven successful in that specific field. The TiO_2 bionanomaterials should be given particular attention so that novel, cost-effective composites can be produced from low-cost feedstock for a sustainable environment. In some research studies, the most common carbonaceous materials like Graphene (G), carbon nanotubes (CNTs), and activated carbon (AC) together with TiO_2 have been evaluated in their free form for water remediation and photodecomposition of pharmaceuticals and personal care products [152] (Fig. 3). Carbonaceous-TiO_2 materials have been proven to exhibit overall better properties than bare TiO_2 based on adsorption capacity, photocatalytic performance, and improved visible light absorption rate [153]. Photocatalytic properties through enhanced sensitivity towards visible light of TiO_2 can be further improved by modifications of titania coupled with carbonaceous elements (Table 5) [154].

In 2019, green synthesis of TiO_2 nanoparticles using *Plumeria acuminata* leaf extracts and subsequent impregnation of silver oxide and boron oxide content on TiO_2 framework to fabricate $Ag_2O/B_2O_3/TiO_2$ nanocomposites has been explored by Tijani et al. Different properties and photocatalytic performance to degrade local dyeing wastewater under artificial and sunlight were compared for undoped TiO_2, Ag_2O/TiO_2, B_2O_3/TiO_2, and $Ag_2O/B_2O_3/TiO_2$ nanocomposite samples. It was reported that the fusion of two oxides to a single spherical particle (coalescence) forming heterojunction enhanced the bond strength in the co-doped TiO_2 than undoped and mono-doped TiO_2 and also the crystallinity and surface area of the ternary oxides as compared to other samples produced, as indicated in Table 5 [155].

Biochar (BC) can act as a support structure for adsorption molecules and as a potent substrate to aid the growth of TiO_2 photocatalyst on its functionalized surface as well [156]. BC being a carbon-rich material is favorable to generating hierarchical structure carbonaceous nanomaterials possessing many surfaces functional groups such as sulfonyl and phenolic groups, and acid complexes, etc. As in Table 5, frequent application to assist in dispersing catalyst nanoparticles is reported owing to its large surface areas, stable structural properties and low-cost decomposition of various pollutants through simultaneous adsorption and degradation is possible through impregnating foreign materials onto BC [157].

Chitosan is a linear polysaccharide that originated from the outer skeleton of shellfish. Given some recent literature, this biomolecule integrated with TiO_2 as nanocomposites has been focused on promising in wastewater treatment as being biodegradable and reinforcing the overall strength in a composite. It was revealed that the chitosan-blended MoO_3–TiO_2 composite boosted photocatalytic degradation towards methylene blue (MB) more than others due to the increased separation of photo-generated charges under the illumination of solar light [158].

Moreover, interestingly, a 3D flowerlike TiO_2 polyaniline (TiO_2/PANI) hybrid was fabricated by a facile sol-gel method. 2D thin PANI nanoflakes were intermeshed within hollow TiO_2 nanoparticles (40–50 nm width, $1 - 2$ μm length) [159]. Chemical oxidation polymerization of aniline in the presence of TiO_2 nanospheres was carried out in an ice bath to prepare a TiO_2/PANI hybrid. TiO_2/PANI composite integrated with a Ti/ANI (aniline) at a molar ratio of 1:1 to fabricate a composite spatial structure (T/P) with a high surface area to show remarkable photocatalytic activities (both UV and solar driven) towards congo red and methyl orange dye molecules (Table 5).
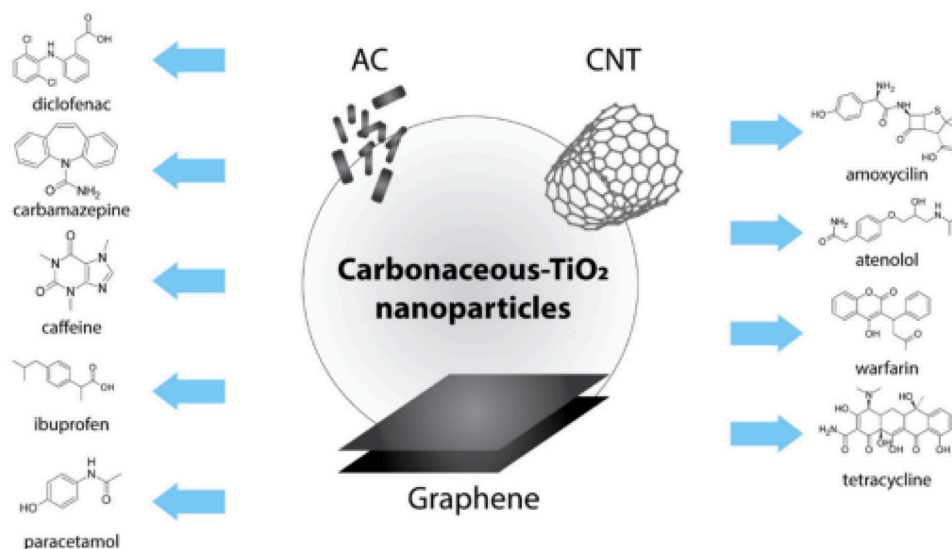
Fig. 3. Photoactivity of carbonaceous-TiO$_2$ nanocomposites as photocatalyst in the decomposition of pharmaceutical pollutants; CNT and AC. [154].

A novel bio-nanocomposite of TiO$_2$ with inulin (a carbohydrate polymer isolated from Allium sativum L) was employed to degrade Methylene blue (MB) dyes under UV light. Electron (e$^-$) and hole (h+) pairs were generated upon UV irradiation on the surface of the nano-composite. The synergistic reinforcement prevented agglomeration of TiO$_2$ in the composite imparting improved photodegradation. Furthermore, Inulin enriched with–OH functionalities assisted in stabilizing the photo-excited electrons, which consequently hindered the recombination with holes as transferred from the conduction band to the surface of inulin [160].

6. Limitations of TiO$_2$

Transition metal oxides have gotten the most attention recently, and titanium dioxide has gained the most attention because of their widespread application in a wide range of areas, including heterogeneous catalysis, gas sensor devices, white pigments, and coating materials. However, it has some drawbacks that limit its application in wastewater (Fig. 4). Brief descriptions are presented as follows.

I. Its range of applications is limited, including solar energy consumption, owing to its small photocatalytic zone (400 nm) and its ability to absorb only about 5% of direct solar irradiation and interior light due to its relatively large bandgap (3–3.2 eV). Therefore, enhancing the photocatalytic activity of TiO$_2$ in the visible range by reducing the bandgap will be required to take advantage of the visible area of the remaining solar spectrum [161,162].

II. Photocatalytic degradation happens largely on the surface of the material. Therefore, when using TiO$_2$ for water treatment, mass transfer limitation must be decreased. However, organic pollutant adsorption on TiO$_2$ surfaces is often minimal due to TiO$_2$'s poor affinity for organic pollutants (mainly hydrophobic organic pollutants), resulting in slow photocatalytic degradation rates [163,164].

III. TiO$_2$ nanoparticles may aggregate during photocatalytic degradation, owing to their instabilities as nanosized particles and the presence of organic ionizable compounds that will link the particles together. As a result, the light incidence on the active centers is reduced, and the catalytic activity of the active centers is diminished [165,166].

IV. The photocatalytic degradation of TiO$_2$ happens largely on the surface, and electron and hole pair transport limitations reduce

photocatalytic performance. Recombination of electrode and hole charge carriers is likely to occur, reducing the material's photocatalytic activity [167].

V. Smaller particles may have lesser photocatalytic activity than larger ones because of higher scattering conditions. Therefore, optimum TiO$_2$ concentration and light wavelengths are essential for photocatalytic activity [72,168].

VI. A crucial issue for the slurry system is recovering nanosized TiO$_2$ particles from treated water, which must be handled for economic and safety reasons [162,168].

VII. There has been a limit to the commercial usage of TiO$_2$ because of the low throughput and expensive cost of photoreactors [169, 170].

7. Organic contaminants degradation in wastewater by using TiO$_2$

TiO2-based photocatalysts have been used effectively over the years to treat various wastewater under various conditions. An overview of the prior studies has been presented in Table 5. Municipal wastewater generally contains a wide range of emerging contaminants. Employing an advanced oxidation process is feasible for municipal wastewater treatment until it is cost-effective and energy-saving. Table 5 shows a novel study focused on N-doped TiO$_2$ to inactivate the antibiotic-resistant *Escherichia coli* strain found in biologically treated urban wastewater. Though the solar photocatalytic treatment caused a decrease in the resistance of *E. coli* to ciprofloxacin and sensitivity to cefuroxime, it could hardly affect the resistance to tetracycline and vancomycin. This process can be applied to small-scale treatment plants to lessen antibiotic resistance and improve the quality of water [171–173].

Unused dyes, surfactants, and trace quantities of heavy metals are usually found in textile wastewater. The factors affecting the removal of dispersed dyes in synthetic wastewater were optimized for the solar-assisted TiO$_2$ process in a study. Although adding H$_2$O$_2$ increases decolorization, the process becomes very sensitive to pH [174]. Another study presented in Table 5 reported the degradation of rhodamine B and mineralization of textile wastewater in the presence of Fe-doped TiO$_2$/rGO nanocomposite under solar illumination. Co-existing anions like chloride and sulfate ions inhibited the degradation process while nitrate and phosphate ions had little influence on decolorization. The composite successfully removed 66.66% total organic carbon (TOC), and 59.1% chemical oxygen demand (COD) from real textile wastewater

Table 5

Summary of wastewater treatment by carbonaceous-TiO_2 nano photocatalysts.

Carbonaceous material integrated TiO_2 nano photocatalyst	Source of biomaterial	Target analyte	Removal efficiency	Remarks	Reference
BC/TiO_2	Microalgae and nutshell	Methyl Orange	90%	2.5 − 3 times higher dye removal after 3 h of treatment with five times drop-casting depositions by both microalgae and nutshell-derived BC-TiO_2 nanocomposites than bare TiO_2 under 100 mW/cm^2 UV light (365 nm)	[257]
BC/TiO_2	Ramie bar	Safranine T	226 mg/g	TiO_2-coated biochar composites displayed excellent adsorptive and photocatalytic efficiency as compared to raw biochar under UV irradiation for 2 h which was also stable enough to reuse after six cycles	[258]
BC/TiO_2 (magnetized)	Papermill sludge	sulfadiazine and oxolinic acid	> 90%	larger antibiotic removal efficiency was observed under solar light for 5 h and 15 min irradiation, mineralizing efficiency was lower than photodegradation performance, magnetization aided the easy separation	[259]
Carbonaceous leaf extracts-$Ag_2O/B_2O_3/TiO_2$	Plumeria acuminate leaf extract	COD, TOC	86.11%, 75.69%	improved and stable photoactivity was due to suppression of recombination reaction of electron-hole with phase conversion of titania under both solar and simulated visible light for 150 min in the order of $Ag_2O/B_2O_3/TiO_2$ >Ag_2O/TiO_2 >TiO_2 >B_2O_3/TiO_2	[155]
Chitosan/MoO_3/TiO_2 (film)	-	Methyl orange	-	improved photocatalytic efficiency was observed due to the increased separation of photo-generated charges under the illumination of solar light for 2 h (TiO_2 < MoO_3− TiO_2 < chitosan< chitosan-blended MoO_3–TiO_2 composite)	[158]
Inulin-TiO_2	Allium sativum L	Methylene blue	92%	synergistic reinforcement prevented agglomeration of TiO_2 in the composite imparting improved photodegradation of dyes under UV exposure	[160]
chitosan/polyacrylic acid/TiO_2	-	Malachite green	91.94%	ultrasonic assisted grafting of acrylic acid onto chitosan coupled with TiO_2 imparted better photodegradation under white light attributed to the catalyst response to the visible region, preventing recombination and introduction of more functional groups	[260]
Cellulose nanocrystals (CNC)/ZnO_2/TiO_2	sawdust	Methylene blue	-	Trapping of UV light was promoted by the CNC matrix and hence greater photocatalytic activities were obtained as the dye molecules were able to infiltrate the inside of the hierarchical hollow spherical structures with efficient charge transfer between ZnO_2 and TiO_2 upon UV exposure	[261]
Carbon nanotube/TiO_2	-	Malachite green	90%	Novel electrostatic adsorption was adopted to combine TiO_2 nanoparticles with a magnetic multi-walled carbon nanotube which enhanced photodegradation under UV exposure for 240 min and assisted magnetic separation for recycling	[262]
TiO_2 nanocrystals/Bi_2O_4	-	Sulfamethoxazole	90%	Effective heterostructure of TiO_2 nanocrystals wrapped-Bi2O4 composites promoted photocatalytic degradation under solar light exposure with 5-cycle stable reusability	[263]
TiO_2/ Polyaniline	-	Congo red, Methyl orange	95%, 83%	3D flowerlike TiO_2 polyaniline (TiO_2/PANI) hybrid exhibited significant photocatalysis performance due to the enhancement of light harvesting and capturing efficiency within the hollow TiO_2 nanosphere and restraining the recombination reaction under UV and sunlight irradiation	[159]
chitosan/TiO_2 @g-C_3N_4	-	methyl orange, rhodamine B, chromium (VI), 2,4-dichloro-phenol and atrazine	90% (overall)	highly reusable chitosan/TiO_2 @g-C3N4 nanocomposite membrane showed significant stability and reusability up to 10 cycles just after an easy water wash each time with improved degradation percentage under visible light and proven to be feasible for continuous-flow system	[264]
TiO_2/g-C_3N_4	-	Phenolic compounds, COD, and dyes	93.06%, 85.62%, 80.23%	TiO_2/g-C3N4 nanocomposite with a band gap of 2.88 eV enhanced the photocatalytic degradation under UV irradiation and the addition of H2O2 accelerated the photocatalytic degradation efficiency due to increased OH radical concentrations.	[265]
chitosan–grafted –poly-Methylaniline imprinted TiO_2	-	Remazol red RB-133	93.50%	chitosan—grafted –poly N-Methylaniline imprinted TiO_2 nanocomposites displayed dual functionality such as sulisunlightven faster self-cleaning photoactivity with 5-cycle stability	[266]
Chitosan/TiO_2/ZnO/graphene	-	tetracycline	> 97%	Novel ternary nanocomposites (T–Z/CS–Gr) were prepared via sol-gel and ultrasound-assisted treatments and imparted the highest degradation efficiency under UV light after 3 h. The molarolar ratio of combination played a vital role in photocatalysis	[267]
TiO_2 (nanofibre)/ graphene	-	Methyl dye	99%	mesoporous TiO_2 nanofibres (TNFs) prepared by electrospinning approach in combination with reduced graphene oxide synergistically enhanced photocatalysis	[268]

Table 5 (*continued*)

| Carbonaceous material integrated TiO$_2$ nano photocatalyst	Source of biomaterial	Target analyte	Removal efficiency	Remarks	Reference
TiO$_2$/graphene	-	Methyl blue, methyl orange	100%, 84%	due to larger surface area, better charge separation, d reduced agglomeration under UV exposure. uniform distribution of the anchored TiO$_2$ nanoparticles on both surfaces of the reduced ced graphene sheet ensured excellent UV-assisted photocatalytic dye degradation	[269]
Graphene quantum dots/ TiO$_2$ nanotube arrays	-	Methylene blue	99.80%	Optimal assembly and interfacial coupling of the hybrid structure graphene quantum dots (GQDs) prepared from carbon fiber by ultrasonic-assisted techniques promoted photodecomposition of dye molecules with a higher surface area of GDQs and lower band gap (3.05 eV) under UV light for 180 min and also stale enough up to 10th recycle.	[270]
Graphene oxide-TiO$_2$ nanorods -Ag	-	Organic dye, phenol, bacteria	100% (120 min), 100% (4 h), 67% (120 min)	multifunctional nanocomposites with large 2D GO sheets, 1D TiO$_2$ nanorods, and 0D Ag nanoparticles ensured the generation of more photocatalytic active sites as well as inhibiting recombination leading to efficient organic dye and phenol/bacterial photodegradation under solar light illumination	[271]
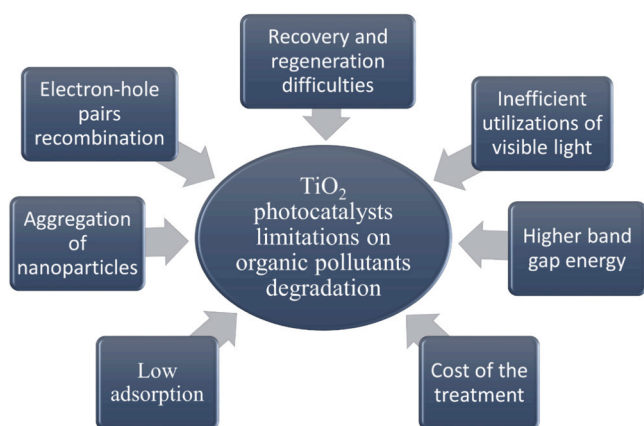
Fig. 4. Limitations of TiO$_2$-based photocatalysts on organic pollutants degradation in wastewater.

in 6.5 h with optimum operating conditions [175]. Stabilized thin films of pure TiO$_2$, N/S-TiO$_2$, and tri-doped N/S/Zn-TiO$_2$ demonstrated practical benefits when applied to treat the azo dyes commonly found in textile effluent along with solar irradiation [35]. TiO$_2$/anthill clay composite was suggested to be a promising low-cost solar photocatalyst for treating textile industry effluent. Even after successive runs, the catalyst showed good stability and reusability against textile dye [37]. Another study investigated the removal of reactive blue 4 dye from textile water with TiO$_2$ photocatalyst using solar energy (Table 6). Additives such as sodium carbonate and sodium chloride hindered the photocatalytic activity, whereas oxidizing agents like hydrogen peroxide and potassium persulfate assisted in photodegradation [176]. ZnO/CdS/TiO$_2$ hybrid effectively degraded atrazine and Rhodamine B [177] and Au-Ag NPs-decorated TiO$_2$-modified Fe$_3$O$_4$ nanocomposite removed Rhodamine 6 G from textile effluent in the presence of solar illumination [36].

Water bodies are being contaminated by tons of pharmaceutical products every year. Conventional wastewater treatment plants cannot degrade pharmaceutical pollutants completely. A study investigated the photocatalytic degradation of ibuprofen under UV and solar radiation. It suggested that TiO$_2$ works better with UV light in acidic conditions [178]. Another study prepared TiO$_2$-carbon microspheres for finding the solar degradation pathway of selected pollutants (diclofenac, acetaminophen, and ibuprofen) in wastewater. The process was very

efficient till five reuse cycles and common inorganic ions could hardly affect the removal efficiency [43]. Pharmaceutically active compounds (PhACs) were successfully degraded by solar-immobilized TiO$_2$ photocatalysis in separate research. This study described water depth as an essential parameter for photodegradation. After photocatalysis, the toxicity of wastewater decreased considerably [179]. From an economical viewpoint, immobilized TiO$_2$ on activated carbon performed better than TiO$_2$ alone. Solar irradiated degradation of amoxicillin, ampicillin, diclofenac, and paracetamol in industrial wastewater depends on pH and catalyst dose [180].

It has become a matter of concern that petroleum refinery uses a large volume of water and releases some harmful chemicals in the produced wastewater. One study has proposed TiO$_2$/ZnO as a solar photocatalyst to keep the COD and TOC of real petroleum wastewater at a standard level. It was observed that bubbling air in the reactor supplies oxygen (O$_2$) to scavenge the photon-produced electrons on the TiO$_2$ and ZnO surfaces [38]. Another study presented in Table 6, analyzed the UV-TiO$_2$ treatment of cooling water found in an oil refinery. It suggested that disinfection efficiency depends on the photocatalyst's effective surface area [181]. When TiO$_2$, ZnO, and H$_2$O$_2$ were applied to real refinery wastewater, TiO$_2$ performed better than ZnO and H$_2$O$_2$. It was also proved that real refinery effluent behaves differently than synthetic industrial wastewater as H$_2$O$_2$ addition decreased the degradation efficiency [182].

TiO$_2$ solar photocatalysis process can treat the pesticides commonly found in wastewater. A study examined four pesticides (Metasystox, Ultracid, Sevnol, and Laition) and observed that TiO$_2$ with solar irradiation can cause the degradation of the active ingredients [183].

The pulp and paper industry are considered a major water pollution source, producing large volumes of toxic wastewater. As presented in Table 6, one study employed sunlight on TiO$_2$ to degrade COD, lignin products, and sulfonated pollutants. It showed that closed circuit performs better with higher COD values due to the accumulation of phenols [184]. In another study, highly contaminated paper mill wastewater was treated with nano-TiO$_2$ to remove COD and TSS present in the effluent. Solar photocatalytic oxidation increases the biodegradability of the wastewater with an increasing BOD$_5$/COD ratio and adding electron acceptors like H$_2$O$_2$ increases the photooxidation efficiency [185].

TiO$_2$ slurry has been reported to inactivate *Cryptosporidium parvum* oocysts in the presence of solar energy. TiO$_2$ coated on glass fibre cloth can remove organic pollutants from sewage water in an environment-friendly method [186]. TiO$_2$ nanopowder with Na$_2$S$_2$O$_8$ can remove bisphenols, phthalates, and parabens from detoxifying wastewater [187].

Table 6

Application of TiO_2 in photocatalytic wastewater treatment.

Photocatalyst	Conditions	Contaminants	Type of Wastewater	Comments	Reference
TiO_2 –WO_3 N-doped TiO_2 Supported TiO_2	Solar pH: 8.3 Time: 120 min Solar Time: 60 min 0.2 g/L Solar Solar 0.01 g/L TiO_2 pH: 6.0	Caffeine Metoprolol Ibuprofen *E. coli* strain N,N-diethyl-m-toluamide (DEET)	Municipal/Urban	Removal: 82% Removal: 91% Removal: 70% Removal: ~100%	[172] [171] [39]
TiO_2 TiO_2/anthill clay Fe-doped TiO_2/rGO nanocomposite TiO_2 ZnO/CdS/TiO_2 hybrid Au-Ag NPs-decorated TiO_2-modified Fe_3O_4 nanocomposite	Solar 2.50 wt% pH: 2.0 Time: 1.07 h Solar 0.6 g/L nanocomposite pH: 6.0 Time: 120 min Solar 2.5 g/L Solar pH: 7 Solar 80 mg photocatalyst Time: 60 min	Dispersed dyes Textile dyes Rhodamine B Reactive Blue 4 Atrazine Rhodamine B Rhodamine-6 G	Textile	Decolorization: 80.17% Decolorization: 70.92% Removal: 91% Removal: 82% Removal: 80% Removal: 90% Removal: ~100%	[174] [37] [175] [176] [177] [36]
TiO_2-carbon microspheres Immobilized TiO_2 Immobilized TiO_2 on activated carbon	Solar pH: 6.0 Time: 3 h Solar 25 g immobilized TiO_2 Time: 96 h Solar pH: 10 0.6 g/L TiO_2	Diclofenac Acetaminophen Ibuprofen Propranolol Diclofenac Carbamazepine Ibuprofen Amoxicillin Ampicillin Diclofenac Paracetamol	Pharmaceutical	Removal: 94% Removal: 65% Removal: 95% Removal: 100% Removal: 100% Removal: 76% Removal: 74% Removal: 100% Removal: 100% Removal: 85% Removal: 70%	[43] [179] [272]
TiO_2/ZnO/Air TiO_2	Solar 0.50 g/L TiO_2 0.54 g/L ZnO 4.3 L/min airflow pH: 6.8 Time: 170 min UV 50 g of TiO2-coated beads Time: 10 min	COD TOC Bacteria	Petroleum refinery Oil refinery	Removal: 74% Removal: 99% Removal: 99.4%	[38] [181]
TiO_2 TiO_2 TiO_2 supported on glass beads TiO_2	Solar 200 mg/L TiO_2 Solar Time: 120 min pH: 3.8 2 g/L TiO_2 Solar Solar 200 mg/L TiO_2	Metasystox, ultracid, sevnol, laition Chlorpyrifos, lambda-cyhalothrin, diazinon Thiabendazole Imazalil, Acetamiprid Diuron, imidacloprid, formetanate, methomyl	Pesticide/agrochemical industry	Removal: 90% COD removal: 79.6% Removal: 100% Order: Diuron>Mythomyl> Imidacloprid>Formetanate	[183] [210] [273] [274]
Nano-TiO_2 TiO_2	Solar 0.75 g/L TiO_2 pH: 6.5 Time: 180 min Solar pH: 3 0.2 g/L TiO_2	COD TSS COD p-toluenesulfonic acid Eugenol Guaiacol	Paper mill	Removal: 70.5% Removal: 80.4% Removal: 20% Removal: 27% Rate constant: 0.0023 min^{-1} Rate constant: 0.0010 min^{-1}	[185] [184]
TiO_2/Sepiolite Graphene-TiO_2	Solar pH: 9.0–11.0 0.8 g/L TiO_2 UV pH: 4 Time: 30 min 3 g/L Gr-TiO_2	Phenol Lignin COD Total phenol Total solid	Olive mill	Removal: 80% Removal: 90% Removal: 88% Removal: 92% Removal: 95%	[275] [188]
TiO_2	UV pH: 4	COD Color	Coffee processing	Removal: 67% Removal: 70%	[40]

(*continued on next page*)

Table 6 (*continued*)

Photocatalyst	Conditions	Contaminants	Type of Wastewater	Comments	Reference
$TiO_2/Fe^{2+}/H_2O_2$	500 mg/L TiO_2 Time: 3 h Solar pH: 7 0.2 g/L TiO_2 0.5 g/L Fe^{2+} 1.35 g/L H_2O_2 UV pH: 6–7 0.5 g/L TiO_2	COD	Hospital	Removal: 99%	[189]
TiO_2 TiO_2 $WO_3/TiO_2/SiO_2$ (WTS)	UV 1 g/L TiO_2 pH: 2.5 (Cr) pH: 10 (CN) UV pH: 9 1.5 g/L WTS 3% (w/w) WO_3 Time: 4 h	Total Carbon (TC) Cr (VI) CN ions Acetaminophen	Organic (synthetic) Synthetic Synthetic	Removal: 58% Removal: 81% Removal: 85% Removal: 95%	[276] [277] [278]

The Olive oil production industry produces highly concentrated wastewater containing nonbiodegradable toxic compounds. For photocatalytic degradation of organic pollutants in olive mill wastewater, important process parameters such as catalyst dose, pH, oxidant concentration, and reaction time were determined using TiO_2/sepiolite nanoparticles. Though solar irradiation provided a cheap and effective method for treating olive mill effluent, the optimum pH range varied for lignin (pH = 9), phenol (pH < 5 and pH > 9–11), and color (pH < 4 and pH > 9) degradation. Another study applied novel graphene-TiO_2 with UV light to remove COD, total phenol, and total solid from olive mill wastewater (Table 6). The process offered high efficiency despite being cost-effective and a 90–95% yield of the catalyst was possible even after six operational cycles [188].

Coffee processing wastewater has become a major environmental concern for developing countries. When solar and UV irradiation were compared for treating real coffee pulping wastewater, it was found that using TiO_2 is more sustainable in countries with high solar irradiance. The study requires detailed investigations to determine the mechanism of pH and oxidant addition on COD and color removal [40].

Hospital wastewater quality must be improved to meet the established standard before mixing with natural water sources. Due to the synergetic effect, the solar/TiO_2/Fe^{2+}/H_2O_2 process was demonstrated as the most efficient method for COD removal from hospital effluent. Moreover, it can reduce treatment time at neutral conditions and less energy consumption [189].

8. Photocatalyst recycling and the concept of circular economy

The biomimetic approach must be included in the design and execution of competitive circular processes in order to meet the four important criteria of ease of use, efficacy, cost-effectiveness, and material availability. Most biological processes rely on the sun for their energy needs, and this is because it is both a renewable resource and a nonpolluting kind of power. As a potential answer to the problems of global energy shortage and environmental degradation, several technologies for transforming solar radiation into chemical fuels, electricity, or heat have attracted much attention. Although photocatalytic treatment's use of solar light to cleanse wastewater is promising, it has encountered significant challenges that need attention. Two major issues with wastewater treatment utilizing photocatalysis are catalyst deactivation after repeated uses and finding a utilization aspect for the produced carbon dioxide. To achieve the goal of a circular economy, there should be a sustainable solution for those issues [190,191].

Many methods for reactivating/deactivating heterogeneous nonphotocatalytic catalysts have been reported and are the topic of ongoing study. Photocatalysts are also susceptible to the same negative consequences of activity degradation. Some reasons for activity loss, including coking and sintering, are absent in photocatalytic water treatment since the process temperatures are so much lower than those in industrial heterogeneous catalytic processes like catalytic hydrogenation, dehydrogenation, and hydrocarbon cracking. The adsorption of oxidation products on the surface of the catalyst is often the cause of activity loss in photocatalytic water treatment [192,193].

The photocatalyst has to be recycled for large-scale applications of photoreactors to be successful. If the catalysts are reused, there will be a significant reduction in the costs associated with the process of treating wastewater. The activity of the catalyst mustn't be decreased significantly between cycles. Depending on the kind and concentration of the pollutant, the amount of activity lost throughout successive use cycles varies. Note that sulfates and other inorganic salts that may be present in a real or simulated wastewater matrix may inhibit photocatalytic activity [194–196].

Multiple techniques exist for separating photocatalyst particles. There are three main separation methods: using a membrane to filter out photocatalyst particles, using a magnet, and using gravity for separation. When a magnetic field is present, the separation efficiency of TiO_2 is improved. Moreover, the photocatalyst can be recycled and recovered with less effort, leading to savings. The catalyst's activity can be restored via regeneration or reactivation. The kind of catalytic poison used is a significant factor in determining the reactivation approach used. The removal of inorganic compounds or low molecular weight organic acids from the photocatalyst's surface may be accomplished by washing with water and aqueous bases. Any organic adsorbate on the TiO_2 surface may be eliminated by (photo)oxidation or treatment with merely the addition of peroxide. The other techniques include heat treatment, irradiation with ultraviolet light, and photooxidation using ultraviolet light. The photocatalytic activity of a deactivated material may often be partially or entirely restored using a thermal reactivation procedure. High temperatures, however, may alter the shape of the catalyst. Around 700 °C, the anatase phase (the most photoactive TiO_2 polymorph) changes crystalline phase to rutile, the less photoactive polymorph. Photocatalysts may be effectively reactivated by thermal and chemical treatment. Ozonation in an aqueous medium was used for chemical reactivation. Higher removal extents were achieved with thermal reactivation, whereas chemical reactivation marginally enhanced photocatalyst stability and biodegradability over reuse cycles [24,193,197].

Numerous studies have shown that the catalyst may be reused up to 4–5 times with just a little decrease in its activity level. However, the catalyst has to be stable (mechanical, crystal structure, chemical, etc.). After being separated from the effluent, the catalysts are then recycled [24]. In the study of Ahmad et al., the prepared photocatalyst was recycled four times and the degradation efficiency in all the cycles was

nearly the same as it was in the first cycle [198]. Sonu et al. investigated the possibility of reusing the sediment component by mixing it with TiO_2 for a few cycles while maintaining the same dye concentration. During this study, the treated supernatant was carefully extracted from the sample, and a fresh untreated sample containing the same amount of dye was added. In order to evaluate the efficacy of the TiO_2 particle sediment alongside the treated dye component, this procedure was investigated in detail. To ensure that sedimented compounds and newly collected samples were properly combined, each sample was thoroughly mixed at a predetermined time interval. Their research demonstrated that the photocatalyst was stable enough to treat dye-infiltrated water for three cycles while maintaining (70−90)% photodegradation efficiency [199]. However, the degradation of the parameters COD, phenol, and TS treated with Graphene-TiO_2 in the Sponza et al. study fell from 95% to 90% after the sixth cycle run [52].

In the context of a circular economy, the "waste to resource" concept revolves around maximizing the utility of materials, minimizing waste, and promoting sustainability. When TiO_2-based catalysts, known for their photocatalytic properties, are employed to treat wastewater containing organic pollutants, the process aligns with circular economy principles. TiO_2 catalysts use light energy to break down harmful organic substances into simpler, less toxic compounds like water and carbon dioxide, effectively purifying the wastewater. During this process, under specific conditions, the breakdown of organic pollutants can lead to the generation of biomass, consisting of microorganisms or organic matter. Instead of considering this biomass as waste, the circular economy mindset views it as a valuable resource. It can be converted into bioenergy, serving as a clean and renewable energy source, or used as a biofertilizer to improve soil quality, reducing the need for chemical fertilizers [200–202]. Microorganisms that are photosynthetic, such as microalgae, are able to create vast quantities of biomass by using only sunshine, carbon dioxide, and a few nutrients. This makes them an excellent source of high-carbon material. Given their high biomass productivity, ability to fix carbon dioxide, and potential for development in saltwater, microalgae, particularly cyanobacteria, are among the most promising choices for bioethanol production. At the moment, everyone is putting their efforts into increasing the production of bioethanol by coming up with a variety of methods to encourage the extraction of carbohydrates from inside the cells. Interestingly, the latter, especially glycogen, may be readily extracted from some cyanobacteria, such as Spirulina platensis, without the need for complicated pretreatments. Since this, these cyanobacteria are prime options for the production of bioethanol [3190,191,203]. Additionally, biomass can be a feedstock for producing bioproducts like bioplastics or pharmaceuticals, fostering a more sustainable and bio-based economy. Fig. 5 depicts the concept of circular economy in TiO_2-based photocatalytic wastewater treatment. The "waste to resource" concept in the circular economy exemplifies sustainability and resource efficiency, minimizing waste while repurposing resources to reduce the environmental impact of wastewater management and organic pollutant remediation.

9. Cost analysis

It is crucial to do economic analyses to verify whether the technology is cost-effective. Cost estimates for water treatment can be carried out in several ways, but all of them include the inclusion of both the total installation costs (i.e., facility cost, project contingency, engineering project, and replacement costs) and the operating expenses (i.e., personnel, maintenance, electricity, and materials and services) [187, 204,205].

Vela et al. used Eq. 14 to calculate the treatment capacity in their study. Using the assumption that the average annual sunshine exposure in their treatment area was about 3000 h and that the useful time (UT) of their pilot plant was set at 480 min per day, they were able to determine
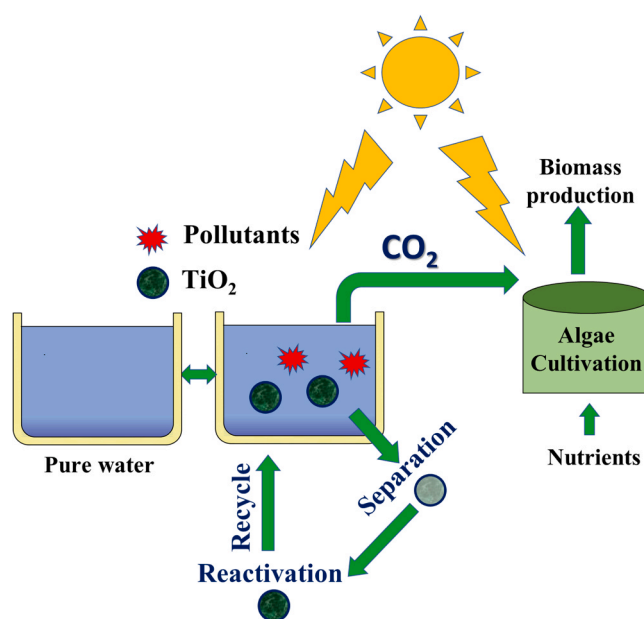

Fig. 5. Concept of circular economy in TiO_2-based photocatalytic wastewater treatment.

the system's treatment capacity (TC).

$$TC = \frac{UT \times V \times 365}{DT90} \, m^3 \bigg/ year \qquad (14)$$

where V is the quantity of water treated (in liters) and DT90 is the time (in minutes) it takes for 90% of the initial pollutant concentration to degrade the chemical that is the most resistant to treatment. Treatment costs were calculated to range from 103 to 285 €/m^3 for photocatalytic treatment using various TiO_2-doped materials, based on an annual work cycle of 365 days at 8 h per day. Considering the bad weather, the price increases to 144–406 €/m^3 if just 240 days of usage are considered. There is a large variation across nations in the average number of hours of sunshine they get annually. For example, average sunshine hours in winter (6.69), summer (6.16), and monsoon (4.81), respectively, demonstrate that Bangladesh has abundant sunlight all year round. Moreover, Scotland gets less than 1200 h of sunshine every year (below 3.3 h per day on average). The quantity of yearly treatments must be drastically decreased as a result [24,206].

Asha et al. researched the viability of real-time livestock wastewater treatment using batch and continuous modes of UV-TiO_2 and granular activated carbon-supported TiO_2 (GAC-TiO_2) photocatalysis systems. Economic analysis was used to analyze the performance in terms of cost and the time needed to reach peak efficiency. Factors such as pollutant type, concentration, contact time, catalyst dosage, and reactor layout were included in the analysis. Power consumption for the magnetic stirrer, pump, aerator, submersible pump, and UV light, if present, are all included in the cost of operation stated in Eqs. 15 and 16. Results showed that experiments in both batch (total operating cost of 0.68 $/kg total volatile solids removal) and continuous (total operational cost of 62.16 $/kg total volatile solids removal) modes using GAC-TiO_2 were extremely effective [207]. Moreover, under ultraviolet light, Balakrishnan studied the degradation of 2,4-dichlorophenoxyacetic acid using chitosan-TiO_2 beads generated using an impregnation process. In order to determine costs, they used the same formulas (Eq. 15 and Eq. 16) as Asha et al. At optimal conditions, they observed that the chitosan-TiO_2 catalyst had a lower overall operational cost (17.7 $ for 2 L treatment) than TiO_2 (22.5 $ for 2 L treatment) [207,208].

$$\text{Total power } consumed(\text{kWh}) = \frac{\text{power } used(\text{W}) \times \text{reaction } time(\text{min})}{1000 \times 60} \quad (15)$$

$$\text{Total operating } cost(\$ \big/ \text{kg}) = \frac{\text{total power } consumed(\text{kWh}) \times \text{unit cost of } power(\$/\text{kWh})}{(\text{initial } concentration - \text{final } concentration) \left(\frac{\text{mg}}{\text{L}}\right) \times \text{working } volume(\text{L})} \times 10^6 \quad (16)$$

Asadi et al. used sol-gel and hydrothermal processes to synthesize highly visible-light photoactive nitrogen and sulfur co-doped TiO$_2$ nanoparticles and nanosheets. Their research found that the sol-gel process was nearly fifty percent less expensive than the hydrothermal method for synthesizing TiO$_2$. Power consumption was 43 kWh for the sol-gel process and 73 kWh for the hydrothermal method, with expenditures of 5.6 and 9.4 \$/kWh, respectively [209]. In another study, TiO$_2$ and TiO$_2$ immobilized on activated carbon (combined process) were evaluated for their ability to degrade four different pharmaceuticals by Alalm et al. In order to estimate expenses, they considered amortization costs of the investments and operational costs per volume of liquid wastewater. TiO$_2$ with activated carbon (combined process) was found to be more cost-effective than TiO$_2$ alone for the removal of all pharmaceuticals from water. In every instance, the cost of amortization was 1.66 \$/m^3, but operating costs ranged from 2.55 \$/m^3 to 3.60 \$/m^3 [180]. However, in another study, they investigated the efficacy of solar photo-Fenton and solar TiO2 photocatalysis processes in the degradation of pesticides in real industrial wastewater. The findings indicate that the estimated cost for photocatalysis (UV/TiO$_2$/H$_2$O$_2$) was 8.69 \$/m^3, whereas photo-Fenton methods incurred costs of 5.2 \$/m^3 [210].

10. Conclusions and future perspectives

Photocatalytic wastewater treatment by nano TiO$_2$ has become both challenging for environmental experts and an exciting new approach to destroying pollutants. It still maintains its importance in contemporary investigations as well as for new ideas due to the unique properties of TiO$_2$ such as the ability to completely decontaminate a wide spectrum of pollutants while also being inexpensive, non-toxic, and requiring a simple experimental design. Although there has been significant research on this topic since the 1970 s, it remains relevant today. In this regard, this paper delves into the key challenges that need to be overcome and the promising avenues that hold the potential to revolutionize wastewater treatment using TiO$_2$-based catalysts. By reviewing recent developments, several approaches can be adopted as the following for future investigations in wastewater treatment:

I. Commercialization and feasibility of the technology for the degradation of different industrial pollutants

II. Innovation, characterization, and application of novel composites by incorporating various technologies, different dopants, co-dopants, other semiconductors, and bio-based materials as well.

III. Innovative reactor designs that maximize wastewater light penetration, catalyst contact, and mass transfer may boost TiO$_2$-based photocatalytic efficiency. Coupling nano TiO$_2$ photocatalysts with different technologies in large-scale water treatment

IV. Comparative study between Solar and artificial light irradiation photoactivity of different photocatalytic composite materials with cost analysis

V. Photocatalytic degradation kinetics

VI. Combining TiO$_2$ photocatalysis with other treatment techniques, such as adsorption or biological processes, may provide hybrid systems with improved efficiency.

VII. The preservation of catalyst stability and durability. TiO$_2$ may have the potential to experience photo corrosion, which may decrease its durability and effectiveness as time progresses.

VIII. Feasibilities of the concept of circular economy in large-scale different industrial pollutants degradation.

IX. Combining TiO$_2$-based photocatalysis with phytoremediation or bioelectrochemical systems may make wastewater treatment comprehensive and sustainable.

X. The continued progress may improve the catalytic activity, selectivity, and stability of TiO$_2$ catalysts in nanotechnology and surface engineering.

Credit author statement

Authors equally contributed to designing and writing the manuscript.

Declaration of Competing Interest

The authors declare that they have no known competing financial interests or personal relationships that could have appeared to influence the work reported in this paper.

Data Availability

The data that has been used is confidential.

Acknowledgments

References

[1] G.B. Mundial, Wastewater? From waste to resource, Waste Glob. Pract. (2020) 1–6 ([Online]. Available), ⟨https://www.worldbank.org/en/topic/water/publication/wastewater-initiative.print⟩.

[2] M.B.K. Suhan, S.B. Shuchi, A. Anis, Z. Haque, M.S. Islam, Comparative degradation study of remazol black B dye using electro-coagulation and electro-Fenton process: Kinetics and cost analysis (Dec), Environ. Nanotechnol., Monit. Manag. 14 (2020), 100335, https://doi.org/10.1016/j.enmm.2020.100335.

[3] A. Serrà, et al., Hybrid Ni@ZnO@ZnS-microalgae for circular economy: a smart route to the efficient integration of solar photocatalytic water decontamination and bioethanol production (Feb), Adv. Sci. 7 (3) (2020) 1902447, https://doi.org/10.1002/advs.201902447.

[4] S. Akter, M.S. Islam, M.H. Kabir, M.A.A. Shaikh, M.A. Gafur, UV/TiO2 photodegradation of metronidazole, ciprofloxacin and sulfamethoxazole in aqueous solution: an optimization and kinetic study (Jul), Arab. J. Chem. 15 (7) (2022), https://doi.org/10.1016/j.arabjc.2022.103900.

[5] S.B. Shuchi, M.B.K. Suhan, S. Bin Humayun, M.E. Haque, M.S. Islam, Heat-activated potassium persulfate treatment of Sudan Black B dye: degradation kinetic and thermodynamic studies (Feb), J. Water Process Eng. 39 (2021), 101690, https://doi.org/10.1016/j.jwpe.2020.101690.

[6] S. Akter, M.B.K. Suhan, M.S. Islam, Recent advances and perspective of electrocoagulation in the treatment of wastewater: a review (May), Environ. Nanotechnol., Monit. Manag. 17 (2022), 100643, https://doi.org/10.1016/j.enmm.2022.100643.

[7] M.B.K. Suhan, S.M.T. Mahtab, W. Aziz, S. Akter, M.S. Islam, Sudan black B dye degradation in aqueous solution by Fenton oxidation process: Kinetics and cost analysis (Dec), Case Stud. Chem. Environ. Eng. 4 (2021), 100126, https://doi.org/10.1016/j.cscee.2021.100126.

[8] M.S. Islam, Y. Zhang, K.N. McPhedran, Y. Liu, M. Gamal El-Din, Granular activated carbon for simultaneous adsorption and biodegradation of toxic oil sands process-affected water organic compounds (Apr), J. Environ. Manag. 152 (2015) 49–57, https://doi.org/10.1016/j.jenvman.2015.01.020.

[9] M.B.K. Suhan, N. Mahmud, M.H.A. Shahria, M.S. Islam, An optimization study of methylene blue dye treatment in synthetic textile wastewater by Fenton oxidation process, J. Chem. Eng. IEB ChE 31 (1) (2023) 75–82.

[10] M.R. Al-Mamun, S. Kader, M.S. Islam, Solar-TiO2 immobilized photocatalytic reactors performance assessment in the degradation of methyl orange dye in aqueous solution (Dec), Environ. Nanotechnol., Monit. Manag. 16 (2021), 100514, https://doi.org/10.1016/j.enmm.2021.100514.

[11] S. Kader, M.R. Al-Mamun, M.B.K. Suhan, S.B. Shuchi, M.S. Islam, Enhanced photodegradation of methyl orange dye under UV irradiation using MoO3 and Ag doped TiO2 photocatalysts, Environ. Technol. Innov. 27 (2022), 102476, https://doi.org/10.1016/j.eti.2022.102476.

[12] P. Yekan Motlagh, A. Khataee, A. Hassani, Y. Orooji, Facile and environmentally friendly synthesis of highly efficient two-dimensional hematene nanosheets for photocatalytic applications (Oct), J. Ind. Eng. Chem. 126 (2023) 465–479, https://doi.org/10.1016/j.jiec.2023.06.035.

[13] A. Hassani, M. Faraji, P. Eghbali, Facile fabrication of mpg-C3N4/Ag/ZnO nanowires/Zn photocatalyst plates for photodegradation of dye pollutant (Sep), J. Photochem. Photobiol. A Chem. 400 (2020), 112665, https://doi.org/10.1016/j.jphotochem.2020.112665.

[14] A.V. Karim, A. Hassani, P. Eghbali, P.V. Nidheesh, Nanostructured modified layered double hydroxides (LDHs)-based catalysts: A review on synthesis, characterization, and applications in water remediation by advanced oxidation processes (Feb), Curr. Opin. Solid State Mater. Sci. 26 (1) (2022), 100965, https://doi.org/10.1016/j.cossms.2021.100965.

[15] S. Riaz, S.-J. Park, An overview of TiO2-based photocatalytic membrane reactors for water and wastewater treatments (Apr), J. Ind. Eng. Chem. 84 (2020) 23–41, https://doi.org/10.1016/j.jiec.2019.12.021.

[16] J. Low, C. Jiang, B. Cheng, S. Wageh, A.A. Al-Ghamdi, J. Yu, A Review of Direct Z-Scheme Photocatalysts (May), Small Methods 1 (5) (2017) 1700080, https://doi.org/10.1002/smtd.201700080.

[17] T. Lopes, P. Dias, L. Andrade, A. Mendes, An innovative photoelectrochemical lab device for solar water splitting (Sep), Sol. Energy Mater. Sol. Cells 128 (2014) 399–410, https://doi.org/10.1016/j.solmat.2014.05.051.

[18] M. Hasan Khan Neon, M.S. Islam, MoO3 and Ag co-synthesized TiO2 as a novel heterogeneous photocatalyst with enhanced visible-light-driven photocatalytic activity for methyl orange dye degradation (July), Environ. Nanotechnol., Monit. Manag. 12 (2019), 100244, https://doi.org/10.1016/j.enmm.2019.100244.

[19] R.J. Clark, G. Felsenfeld "© 1972 Nature Publishing Group Nat. N. Biol. 240 1972 226 229 doi: 10.1038/239137a0.

[20] S.N. Frank, A.J. Bard, Heterogeneous photocatalytic oxidation of cyanide ion in aqueous solutions at TiO2 powder, J. Am. Chem. Soc. 99 (1) (1977) 303–304, https://doi.org/10.1021/ja00443a081.

[21] S. Horikoshi, N. Serpone, Can the photocatalyst TiO2 be incorporated into a wastewater treatment method? Background and prospects, Catal. Today 340 (2020) 334–346, https://doi.org/10.1016/j.cattod.2018.10.020.

[22] M.J. Martín de Vidales, et al., 3D printed floating photocatalysts for wastewater treatment, Catal. Today 328 (2019) 157–163, https://doi.org/10.1016/j.cattod.2019.01.074.

[23] R. Singh, S. Dutta, Synthesis and characterization of solar photoactive TiO2 nanoparticles with enhanced structural and optical properties, Adv. Powder Technol. 29 (2) (2018) 211–219, https://doi.org/10.1016/j.apt.2017.11.005.

[24] S. Dutta, Wastewater treatment using TiO2-based photocatalysis, L. INC, 2020.

[25] S.M. Pasini, et al., An overview on nanostructured TiO2–containing fibers for photocatalytic degradation of organic pollutants in wastewater treatment (Apr), J. Water Process Eng. 40 (2021), 101827, https://doi.org/10.1016/j.jwpe.2020.101827.

[26] Y. Wang, Y. He, Q. Lai, M. Fan, Review of the progress in preparing nano TiO2: An important environmental engineering material (Nov), J. Environ. Sci. 26 (11) (2014) 2139–2177, https://doi.org/10.1016/j.jes.2014.09.023.

[27] F. Pellegrino, et al., Influence of agglomeration and aggregation on the photocatalytic activity of TiO 2 nanoparticles (Nov), Appl. Catal. B Environ. 216 (2017) 80–87, https://doi.org/10.1016/j.apcatb.2017.05.046.

[28] J. Melcher, N. Barth, C. Schilde, A. Kwade, D. Bahnemann, Influence of TiO2 agglomerate and aggregate sizes on photocatalytic activity (Jan), J. Mater. Sci. 52 (2) (2017) 1047–1056, https://doi.org/10.1007/s10853-016-0400-z.

[29] V. Etacheri, C. Di Valentin, J. Schneider, D. Bahnemann, S.C. Pillai, Visible-light activation of TiO2 photocatalysts: Advances in theory and experiments (Dec), J. Photochem. Photobiol. C. Photochem. Rev. 25 (2015) 1–29, https://doi.org/10.1016/j.jphotochemrev.2015.08.003.

[30] M.B.K. Suhan, S.B. Shuchi, M.R. Al-Mamun, H. Roy, M.S. Islam, Enhanced UV light-driven photocatalytic degradation of methyl orange using MoO3/WO3-fluorinated TiO2 nanocomposites (May), Environ. Nanotechnol., Monit. Manag. 19 (2023), 100768, https://doi.org/10.1016/j.enmm.2022.100768.

[31] Z. Huang, H. Liu, Insights into the pathways, intermediates, influence factors and toxicological properties in the degradation of tetracycline by TiO2-based photocatalysts (Oct), J. Environ. Chem. Eng. 11 (5) (2023), 110587, https://doi.org/10.1016/j.jece.2023.110587.

[32] J. Moma, J. Baloyi, Modified Titanium Dioxide for Photocatalytic Applications. Photocatalysts - Applications and Attributes, IntechOpen,, 2019.

[33] M.R. Al-Mamun, S. Kader, M.S. Islam, M.Z.H. Khan, Photocatalytic activity improvement and application of UV-TiO2 photocatalysis in textile wastewater treatment: A review (Oct), J. Environ. Chem. Eng. 7 (5) (2019), 103248, https://doi.org/10.1016/j.jece.2019.103248.

[34] B. Muzikova, et al., Composite TiO2-based photocatalyst with enhanced performance (Sep), Photochem. Photobiol. Sci. 22 (1) (2022) 73–86, https://doi.org/10.1007/s43630-022-00300-5.

[35] R. Foulady-Dehaghi, M. Behpour, Visible and solar photodegradation of textile wastewater by multiple doped TiO2/Zn nanostructured thin films in fixed bed photoreactor mode, Inorg. Chem. Commun. 117 (March) (2020), 107946, https://doi.org/10.1016/j.inoche.2020.107946.

[36] M. Amoli-Diva, A. Anvari, R. Sadighi-Bonabi, Synthesis of magneto-plasmonic Au-Ag NPs-decorated TiO2-modified Fe3O4 nanocomposite with enhanced laser/solar-driven photocatalytic activity for degradation of dye pollutant in textile wastewater, Ceram. Int. 45 (14) (2019) 17837–17846, https://doi.org/10.1016/j.ceramint.2019.05.355.

[37] A.S. Yusuff, I.I. Olateju, O.A. Adesina, TiO2/anthill clay as a heterogeneous catalyst for solar photocatalytic degradation of textile wastewater: Catalyst characterization and optimization studies, Materialia 8 (September) (2019), 100484, https://doi.org/10.1016/j.mtla.2019.100484.

[38] D. al deen, A. Aljuboury, F. Shaik, Optimization of the petroleum wastewater treatment process using TiO2/Zn photocatalyst, South Afr. J. Chem. Eng. 38 (January) (2021) 61–69, https://doi.org/10.1016/j.sajce.2021.08.001.

[39] E.M. Rodríguez, A. Rey, E. Mena, F.J. Beltrán, Application of solar photocatalytic ozonation in water treatment using supported TiO2, Appl. Catal. B Environ. 254 (April) (2019) 237–245, https://doi.org/10.1016/j.apcatb.2019.04.095.

[40] G. Sujatha, G. Shanthakumar, F. Chiampo, UV light-irradiated photocatalytic degradation of coffee processing wastewater using tio2 as a catalyst, Environ. -MDPI 7 (6) (2020) 1–13, https://doi.org/10.3390/environments7060047.

[41] E.H. Rdewi, K.K. Abbas, A.M.H. AbdulkadhimAl-Ghaban, Removal pharmaceutical carbamazepine from wastewater using ZnO-TiO2-MXene heterostructural nanophotocatalyst under solar light irradiation, Mater. Today Proc. 60 (2022) 1702–1711, https://doi.org/10.1016/j.matpr.2021.12.229.

[42] O.F.S. Khasawneh, P. Palaniandy, P. Palaniandy, M. Ahmadipour, H. Mohammadi, and M. R. Bin Hamdan, "Removal of acetaminophen using Fe2O3-TiO2nanocomposites by photocatalysis under simulated solar irradiation: Optimization study, J. Environ. Chem. Eng. 9 (1) (2021), 104921, https://doi.org/10.1016/j.jece.2020.104921.

[43] M. Peñas-Garzón, W.H.M. Abdelraheem, C. Belver, J.J. Rodriguez, J. Bedia, D. D. Dionysiou, TiO2-carbon microspheres as photocatalysts for effective remediation of pharmaceuticals under simulated solar light, Sep. Purif. Technol. 275 (2021), https://doi.org/10.1016/j.seppur.2021.119169.

[44] I.J. Ani, U.G. Akpan, M.A. Olutoye, B.H. Hameed, Photocatalytic degradation of pollutants in petroleum refinery wastewater by TiO2- and ZnO-based photocatalysts: Recent development, J. Clean. Prod. 205 (2018) 930–954, https://doi.org/10.1016/j.jclepro.2018.08.189.

[45] Z. Ghasemi, H. Younesi, A.A. Zinatizadeh, Preparation, characterization and photocatalytic application of TiO2/Fe-ZSM-5 nanocomposite for the treatment of petroleum refinery wastewater: Optimization of process parameters by response surface methodology, Chemosphere 159 (2016) 552–564, https://doi.org/10.1016/j.chemosphere.2016.06.058.

[46] S. Kalidhasan, H.-Y. Lee, Preparation of TiO2-deposited silica-based catalysts for photocatalytic decomposition of chloro-pesticide to environmentally less toxic species (Mar), Chemosphere 290 (2022), 133300, https://doi.org/10.1016/j.chemosphere.2021.133300.

[47] A. Sraw, T. Kaur, I. Thakur, A. Verma, R.K. Wanchoo, A.P. Toor, Photocatalytic degradation of pesticide monocrotophos in water using W-TiO2 in slurry and fixed bed recirculating reactor (Oct), J. Mol. Struct. 1265 (2022), 133392, https://doi.org/10.1016/j.molstruc.2022.133392.

[48] H. Esfandian, Z. Beiramzadeh, E. Shekarian, R. Katal, Improvement in biodegradability of paper mill wastewater by anatase TiO2 predominant in {001} facet in the batch and packed bed photoreactor (PBPR) (Nov), Int. J. Environ. Sci. Technol. 18 (11) (2021) 3441–3448, https://doi.org/10.1007/s13762-020-03094-0.

[49] Y.-M. Chu, Q.-V. Bach, Application of TiO2 nanoparticle for solar photocatalytic oxidation system (Nov), Appl. Nanosci. (2020), https://doi.org/10.1007/s13204-020-01614-5.

[50] S. Puri, A. Verma, Color removal from secondary treated pulp & paper industry effluent using waste driven Fe–TiO2 composite (Sep), Chemosphere 303 (2022), 135143, https://doi.org/10.1016/j.chemosphere.2022.135143.

[51] A. Mancuso, et al., Solar driven photocatalysis using iron and chromium doped TiO2 coupled to moving bed biofilm process for olive mill wastewater treatment (Dec), Chem. Eng. J. 450 (2022) 138107, https://doi.org/10.1016/j.cej.2022.138107.

[52] D.T. Sponza, P. Koyuncuoglu, and C. Ulusoy, "Photo degradation of Olive Mill Wastewaters Using Graphene-Tio2 and Recovery of Graphene-Tio 2," 10, 8, pp. 424–432, 2022.

[53] S. Sanguanpak, W. Shongkittikul, C. Saengam, C. Chiemchaisri, C. Chiemchaisri, TiO2-immobilized porous geopolymer composite membrane for removal of antibiotics in hospital wastewater (Nov), Chemosphere 307 (2022), 135760, https://doi.org/10.1016/j.chemosphere.2022.135760.

[54] S. Teixeira, P.M. Martins, S. Lanceros-Méndez, K. Kühn, G. Cuniberti, Reusability of photocatalytic TiO2 and ZnO nanoparticles immobilized in poly(vinylidene

difluoride)-co-trifluoroethylene (Oct), Appl. Surf. Sci. 384 (2016) 497–504, https://doi.org/10.1016/j.apsusc.2016.05.073.

[55] Z. Al-Qodah, et al., Sustainable vs. Conventional Approach for Olive Oil Wastewater Management: A Review of the State of the Art (May), Water 14 (11) (2022) 1695, https://doi.org/10.3390/w14111695.

[56] R. Katal, S. Masudy-Panah, M. Tanhaei, M.H.D.A. Farahani, H. Jiangyong, A review on the synthesis of the various types of anatase TiO2 facets and their applications for photocatalysis (Mar), Chem. Eng. J. 384 (2020), 123384, https://doi.org/10.1016/j.cej.2019.123384.

[57] G. Li, et al., Surface study of the reconstructed anatase TiO2 (001) surface (Feb), Prog. Nat. Sci. Mater. Int. 31 (1) (2021) 1–13, https://doi.org/10.1016/j.pnsc.2020.11.002.

[58] B.A. van Driel, P.J. Kooyman, K.J. van den Berg, A. Schmidt-Ott, J. Dik, A quick assessment of the photocatalytic activity of TiO2 pigments — From lab to conservation studio! (May), Microchem. J. 126 (2016) 162–171, https://doi.org/10.1016/j.microc.2015.11.048.

[59] H. Park, Y. Park, W. Kim, W. Choi, Surface modification of TiO2 photocatalyst for environmental applications (Jun), J. Photochem. Photobiol. C. Photochem. Rev. 15 (2013) 1–20, https://doi.org/10.1016/j.jphotochemrev.2012.10.001.

[60] A.G. Akerdi, S.H. Bahrami, Application of heterogeneous nano-semiconductors for photocatalytic advanced oxidation of organic compounds: A review, J. Environ. Chem. Eng. 7 (5) (2019), 103283, https://doi.org/10.1016/j.jece.2019.103283.

[61] G. Varshney, et al., Nanoscale TiO2 films and their application in remediation of organic pollutants, Coord. Chem. Rev. 306 (P1) (2016) 43–64, https://doi.org/10.1016/j.ccr.2015.06.011.

[62] A. Amalraj, A. Pius, Photocatalytic degradation of monocrotophos and chlorpyrifos in aqueous solution using TiO2 under UV radiation, J. Water Process Eng. 7 (2015) 94–101, https://doi.org/10.1016/j.jwpe.2015.06.002.

[63] Q.E. Zhao, W. Wen, Y. Xia, J.M. Wu, Photocatalytic activity of TiO2 nanorods, nanowires and nanoflowers filled with TiO2 nanoparticles, December 2017, Thin Solid Films 648 (2018) 103–107, https://doi.org/10.1016/j.tsf.2018.01.004.

[64] J. Yu, J. Lei, L. Wang, J. Zhang, Y. Liu, TiO2 inverse opal photonic crystals: Synthesis, modification, and applications - A review, J. Alloy. Compd. 769 (2018) 740–757, https://doi.org/10.1016/j.jallcom.2018.07.357.

[65] P. Punia, et al., Recent advances in synthesis, characterization, and applications of nanoparticles for contaminated water treatment- A review, Ceram. Int. 47 (2) (2021) 1526–1550, https://doi.org/10.1016/j.ceramint.2020.09.050.

[66] X.-Z. Wei, H. Wang, B. Xu, C. Shen, J. Liu, L. Ma, Efficient visible light-driven oxidation of bio-1-butanol over a TiO2-based photocatalyst system, Colloids Surf. A Physicochem. Eng. Asp. 665 (2023), 131216, https://doi.org/10.1016/j.colsurfa.2023.131216.

[67] T. Gupta, Samriti, J. Cho, J. Prakash, Hydrothermal synthesis of TiO2 nanorods: formation chemistry, growth mechanism, and tailoring of surface properties for photocatalytic activities, Mater. Today Chem. 20 (2021), 100428, https://doi.org/10.1016/j.mtchem.2021.100428.

[68] S. Merabet, A. Bouzaza, D. Wolbert, Photocatalytic degradation of indole in a circulating upflow reactor by UV/TiO2 process-Influence of some operating parameters, J. Hazard. Mater. 166 (2–3) (2009) 1244–1249, https://doi.org/10.1016/j.jhazmat.2008.12.047.

[69] N. Madkhali, et al., Recent update on photocatalytic degradation of pollutants in waste water using TiO2-based heterostructured materials, Results Eng. 17 (2023), 100920, https://doi.org/10.1016/j.rineng.2023.100920.

[70] M.R. Al-Mamun, S. Kader, M.S. Islam, M.Z.H. Khan, Photocatalytic activity improvement and application of UV-TiO2 photocatalysis in textile wastewater treatment: A review, J. Environ. Chem. Eng. 7 (5) (2019), 103248, https://doi.org/10.1016/j.jece.2019.103248.

[71] M.E. Borges, M. Sierra, E. Cuevas, R.D. García, P. Esparza, Photocatalysis with solar energy: Sunlight-responsive photocatalyst based on TiO2 loaded on a natural material for wastewater treatment, Sol. Energy 135 (2016) 527–535, https://doi.org/10.1016/J.SOLENER.2016.06.022.

[72] D. Chen, et al., Photocatalytic degradation of organic pollutants using TiO2-based photocatalysts: A review, J. Clean. Prod. 268 (2020), 121725, https://doi.org/10.1016/j.jclepro.2020.121725.

[73] S. Bagwasi, B. Tian, J. Zhang, M. Nasir, Synthesis, characterization and application of bismuth and boron-doped TiO2: A visible light active photocatalyst, Chem. Eng. J. 217 (2013) 108–118, https://doi.org/10.1016/J.CEJ.2012.11.080.

[74] M.R. Al-Mamun, S. Kader, M.S. Islam, M.Z.H. Khan, Photocatalytic activity improvement and application of UV-TiO2 photocatalysis in textile wastewater treatment: A review (Oct), J. Environ. Chem. Eng. 7 (5) (2019), 103248, https://doi.org/10.1016/J.JECE.2019.103248.

[75] A. Rani, R.L. Dhiman, V. Singh, S. Kumar, S. Kumar, Photocatalytic study of Ni-N-codoped TiO2nanoparticles under visible light irradiation, Nano Express 2 (3) (2021), https://doi.org/10.1088/2632-959X/abe058.

[76] S.P. Keerthana, R. Yuvakkumar, G. Ravi, S.I. Hong, A.G. Al-Sehemi, D. Velauthapillai, Fabrication of Ce doped TiO2 for efficient organic pollutants removal from wastewater, December 2021, Chemosphere 293 (2022), 133540, https://doi.org/10.1016/j.chemosphere.2022.133540.

[77] X. Zhu, L. Pei, R. Zhu, Y. Jiao, R. Tang, W. Feng, Preparation and characterization of Sn/La co-doped TiO2 nanomaterials and their phase transformation and photocatalytic activity, Sci. Rep. 8 (1) (2018) 1–14, https://doi.org/10.1038/s41598-018-30050-3.

[78] C. Thambiliyagodage, L. Usgodaarachchi, Photocatalytic activity of N, Fe and Cu co-doped TiO2 nanoparticles under sunlight, Curr. Res. Green. Sustain. Chem. 4 (2021), 100186, https://doi.org/10.1016/J.CRGSC.2021.100186.

[79] R. Sinha, P.S. Ghosal, A comprehensive appraisal on status and management of remediation of DBPs by TiO2 based-photocatalysts: Insights of technology, performance and energy efficiency (Feb), J. Environ. Manag. 328 (2023), 117011, https://doi.org/10.1016/j.jenvman.2022.117011.

[80] A. Rafiq, et al., Photocatalytic degradation of dyes using semiconductor photocatalysts to clean industrial water pollution, J. Ind. Eng. Chem. 97 (2021) 111–128, https://doi.org/10.1016/j.jiec.2021.02.017.

[81] A. K, G. P, Photodegradation of methyl orange in aqueous solution by the visible light active Co:La:TiO2 nanocomposite, Chem. Sci. J. 08 (03) (2017) 1000164, https://doi.org/10.4172/2150-3494.1000164.

[82] H. Zhu, et al., Effective photocatalytic decolorization of methyl orange utilizing TiO 2/ZnO/chitosan nanocomposite films under simulated solar irradiation, Desalination 286 (2012) 41–48, https://doi.org/10.1016/j.desal.2011.10.036.

[83] E.C. Ilinoiu, et al., Photocatalytic activity of a nitrogen-doped TiO2 modified zeolite in the degradation of Reactive Yellow 125 azo dye, J. Taiwan Inst. Chem. Eng. 44 (2) (2013) 270–278, https://doi.org/10.1016/j.jtice.2012.09.006.

[84] M.R. Al-Mamun, M.N. Karim, N.A. Nitun, S. Kader, M.S. Islam, M.Z.H. Khan, Photocatalytic performance assessment of GO and Ag co-synthesized TiO2 nanocomposite for the removal of methyl orange dye under solar irradiation, Environ. Technol. Innov. 22 (2021), 101537, https://doi.org/10.1016/j.eti.2021.101537.

[85] R. Ahmad, Z. Ahmad, A.U. Khan, N.R. Mastoi, M. Aslam, J. Kim, Photocatalytic systems as an advanced environmental remediation: Recent developments, limitations and new avenues for applications, J. Environ. Chem. Eng. 4 (4) (2016) 4143–4164, https://doi.org/10.1016/j.jece.2016.09.009.

[86] M.A. Rauf, M.A. Meetani, S. Hisaindee, An overview on the photocatalytic degradation of azo dyes in the presence of TiO2 doped with selective transition metals, Desalination 276 (1–3) (2011) 13–27, https://doi.org/10.1016/j.desal.2011.03.071.

[87] M. Muruganandham, M. Swaminathan, TiO2-UV photocatalytic oxidation of Reactive Yellow 14: Effect of operational parameters, J. Hazard. Mater. 135 (1–3) (2006) 78–86, https://doi.org/10.1016/j.jhazmat.2005.11.022.

[88] Y. Çalışkan, H.C. Yatmaz, N. Bektaş, Photocatalytic oxidation of high concentrated dye solutions enhanced by hydrodynamic cavitation in a pilot reactor, Process Saf. Environ. Prot. 111 (2017) 428–438, https://doi.org/10.1016/j.psep.2017.08.003.

[89] K. Hathaisamit, W. Sutha, P. Kamruang, S. Pudwat, S. Teekasap, Decolorization of cationic yellow X-Gl 200% from textile dyes by TiO 2 films-coated rotor, Procedia Eng. 32 (2012) 800–806, https://doi.org/10.1016/j.proeng.2012.02.015.

[90] J.L. Shie, C.H. Lee, C.S. Chiou, C.T. Chang, C.C. Chang, C.Y. Chang, Photodegradation kinetics of formaldehyde using light sources of UVA, UVC and UVLED in the presence of composed silver titanium oxide photocatalyst, J. Hazard. Mater. 155 (1–2) (2008) 164–172, https://doi.org/10.1016/j.jhazmat.2007.11.043.

[91] T.S. Natarajan, M. Thomas, K. Natarajan, H.C. Bajaj, R.J. Tayade, Study on UV-LED/TiO2 process for degradation of Rhodamine B dye, Chem. Eng. J. 169 (1–3) (2011) 126–134, https://doi.org/10.1016/j.cej.2011.02.066.

[92] R. Mariselvam, A.J.A. Ranjitsingh, P. Mosae Selvakumar, A.A. Alarfaj, M. A. Munusamy, Spectral studies of UV and solar photocatalytic degradation of AZO dye and textile dye effluents using green synthesized silver nanoparticles, Bioinorg. Chem. Appl. 2016 (2016) 1–9, https://doi.org/10.1155/2016/8629178.

[93] K.V.S. Rao, M. Subrahmanyam, P. Boule, Immobilized TiO2 photocatalyst during long-term use: decrease of its activity, Appl. Catal. B Environ. 49 (4) (2004) 239–249, https://doi.org/10.1016/j.apcatb.2003.12.017.

[94] A. Bouarioua, M. Zerdaoui, Photocatalytic activities of TiO2 layers immobilized on glass substrates by dip-coating technique toward the decolorization of methyl orange as a model organic pollutant, J. Environ. Chem. Eng. 5 (2) (2017) 1565–1574, https://doi.org/10.1016/j.jece.2017.02.025.

[95] W.Z. Tang, Huren An, UV/TiO2 photocatalytic oxidation of commercial dyes in aqueous solutions, Chemosphere 31 (9) (1995) 4157–4170, https://doi.org/10.1016/0045-6535(95)80015-D.

[96] I.K. Konstantinou, T.A. Albanis, TiO2-assisted photocatalytic degradation of azo dyes in aqueous solution: Kinetic and mechanistic investigations: A review, Appl. Catal. B Environ. 49 (1) (2004) 1–14, https://doi.org/10.1016/j.apcatb.2003.11.010.

[97] M. Muruganandham, M. Swaminathan, Photocatalytic decolourisation and degradation of Reactive Orange 4 by TiO2-UV process, Dye. Pigment. 68 (2–3) (2006) 133–142, https://doi.org/10.1016/j.dyepig.2005.01.004.

[98] M.M. Rashid, B. Simončič, B. Tomšič, Recent advances in TiO2-functionalized textile surfaces, Surf. Interfaces 22 (2021), 100890, https://doi.org/10.1016/j.surfin.2020.100890.

[99] X. Hu, et al., Mechanisms underlying degradation pathways of microcystin-LR with doped TiO2 photocatalysis, Chem. Eng. J. 330 (May) (2017) 355–371, https://doi.org/10.1016/j.cej.2017.07.161.

[100] Y. Zhang, et al., Photoelectrocatalytic degradation of recalcitrant organic pollutants using TiO2 film electrodes: An overview, Chemosphere 88 (2) (2012) 145–154, https://doi.org/10.1016/j.chemosphere.2012.03.020.

[101] K. Bubacz, B. Tryba, A.W. Morawski, The role of adsorption in decomposition of dyes on TiO 2 and N-modified TiO 2 photocatalysts under UV and visible light irradiations, Mater. Res. Bull. 47 (11) (2012) 3697–3703, https://doi.org/10.1016/j.materresbull.2012.06.038.

[102] M. Rafique, et al., Hydrogen Production Using TiO 2 -Based Photocatalysts: A Comprehensive Review (Jul), ACS Omega 8 (29) (2023) 25640–25648, https://doi.org/10.1021/acsomega.3c00963.

[103] A. Khlyustova, N. Sirotkin, T. Kusova, A. Kraev, V. Titov, A. Agafonov, Doped TiO 2: the effect of doping elements on photocatalytic activity, Mater. Adv. 1 (5) (2020) 1193–1201, https://doi.org/10.1039/D0MA00171F.

[104] R. Jaiswal, N. Patel, D.C. Kothari, A. Miotello, Improved visible light photocatalytic activity of TiO2 co-doped with Vanadium and Nitrogen, Appl. Catal. B Environ. 126 (2012) 47–54, https://doi.org/10.1016/J.APCATB.2012.06.030.

[105] M.A. Lazar, S. Varghese, and S.S. Nair, Photocatalytic water treatment by titanium dioxide: Recent updates, 2, 4. 2012.

[106] M.R.D. Khaki, M.S. Shafeeyan, A.A.A. Raman, W.M.A.W. Daud, Application of doped photocatalysts for organic pollutant degradation - A review, J. Environ. Manag. 198 (2017) 78–94, https://doi.org/10.1016/j.jenvman.2017.04.099.

[107] G. Pedroza-Herrera, I.E. Medina-Ramírez, J.A. Lozano-Álvarez, S.E. Rodil, Evaluation of the Photocatalytic Activity of Copper Doped TiO2 nanoparticles for the Purification and/or Disinfection of Industrial Effluents (Feb), Catal. Today 341 (2020) 37–48, https://doi.org/10.1016/J.CATTOD.2018.09.017.

[108] S. Sood, A. Umar, S.K. Mehta, S.K. Kansal, Highly effective Fe-doped TiO 2 nanoparticles photocatalysts for visible- light driven photocatalytic degradatio, J. Colloid Interface Sci. 450 (2015) 213–323.

[109] R. Chauhan, A. Kumar, R.P. Chaudhary, Structural and photocatalytic studies of Mn doped TiO2 nanoparticles (Dec), Spectrochim. Acta Part A Mol. Biomol. Spectrosc. 98 (2012) 256–264, https://doi.org/10.1016/J.SAA.2012.08.009.

[110] M.A. Barakat, R.I. Al-Hutailah, E. Qayyum, J.N. Kuhn, Pt-Doped TiO2 nanoparticles for photocatalytic degradation of phenols in wastewater, REWAS 2013 Enabling Mater. Resour. Sustain (2013) 309–322, https://doi.org/10.1002/9781118679401.ch31.

[111] D.V. Aware, S.S. Jadhav, Synthesis, characterization and photocatalytic applications of Zn-doped TiO2 nanoparticles by sol–gel method, Appl. Nanosci. 6 (7) (2016) 965–972, https://doi.org/10.1007/s13204-015-0513-8.

[112] S. Mugundan, et al., Sol-gel synthesized barium doped TiO2 nanoparticles for solar photocatalytic application (May), Inorg. Chem. Commun. 139 (2022), 109340, https://doi.org/10.1016/J.INOCHE.2022.109340.

[113] S. Mugundan, B. Rajamannan, G. Viruthagiri, N. Shanmugam, R. Gobi, P. Praveen, Synthesis and characterization of undoped and cobalt-doped TiO2 nanoparticles via sol–gel technique, Appl. Nanosci. 5 (4) (2015) 449–456, https://doi.org/10.1007/s13204-014-0337-y.

[114] M.A. Barakat, H. Schaeffer, G. Hayes, S. Ismat-Shah, Photocatalytic degradation of 2-chlorophenol by Co-doped TiO2 nanoparticles, Appl. Catal. B Environ. 57 (1) (2005) 23–30, https://doi.org/10.1016/j.apcatb.2004.10.001.

[115] K.T. Kubra, M.S. Salman, M.N. Hasan, Enhanced toxic dye removal from wastewater using biodegradable polymeric natural adsorbent, J. Mol. Liq. 328 (2021), 115468, https://doi.org/10.1016/j.molliq.2021.115468.

[116] M. Nasr, C. Eid, R. Habchi, P. Miele, M. Bechelany, Recent Progress on Titanium Dioxide Nanomaterials for Photocatalytic Applications, ChemSusChem 11 (18) (2018) 3023–3047, https://doi.org/10.1002/cssc.201800874.

[117] S. Yu, et al., Recent advances in metal-organic framework membranes for water treatment: A review (Dec), Sci. Total Environ. 800 (2021), 149662, https://doi.org/10.1016/J.SCITOTENV.2021.149662.

[118] C.K. Foo, et al., Density and viscosity of aqueous mixtures of N-methyldiethanolamines (MDEA), piperazine (PZ) and ionic liquids (Sep), J. Mol. Liq. 209 (2015) 596–602, https://doi.org/10.1016/J.MOLLIQ.2015.05.041.

[119] M.N. Hasan, M.S. Salman, A. Islam, H. Znad, M.M. Hasan, Sustainable composite sensor material for optical cadmium(II) monitoring and capturing from wastewater, Microchem. J. 161 (2021), 105800, https://doi.org/10.1016/j.microc.2020.105800.

[120] M.S. Salman, H. Znad, M.N. Hasan, M.M. Hasan, Optimization of innovative composite sensor for Pb(II) detection and capturing from water samples, Microchem. J. 160 (2021), 105765, https://doi.org/10.1016/j.microc.2020.105765.

[121] C. Yan, K.F. Chen, C.H. Lai, S.W. Lai, Q. Chang, Y.P. Peng, Photocatalytic degradation of Rhodamine B by microwave-assisted hydrothermal synthesized N-doped titanate nanotubes, J. Environ. Sci. 26 (7) (2014) 1505–1512, https://doi.org/10.1016/J.JES.2014.05.017.

[122] M.S. Azami, W.I. Nawawi, A.H. Jawad, M.A.M. Ishak, K. Ismail, N-doped TiO2 synthesised via microwave induced photocatalytic on RR4 dye removal under LED light irradiation, Sains Malays. 46 (8) (2017) 1309–1316, https://doi.org/10.17576/jsm-2017-4608-17.

[123] K. Siuzdak, M. Szkoda, M. Sawczak, A. Lisowska-Oleksiak, Novel nitrogen precursors for electrochemically driven doping of titania nanotubes exhibiting enhanced photoactivity, N. J. Chem. 39 (4) (2015) 2741–2751, https://doi.org/10.1039/c5nj00127g.

[124] S. Wang et al., Removal of Antibiotic Resistant Bacteria and Genes by UV-Assisted Electrochemical Oxidation on Degenerative TiO 2 Nanotube Arrays (Mar), ACS EST Eng. 1 (3) (2021) 612–622, https://doi.org/10.1021/acsestengg.1c00011.

[125] D. Cao, et al., Enhanced the photoelectrocatalytic performance of TiO2 nanotube arrays by the synergistic sensitization of Ag–AgBr nanospheres (Feb), Spectrochim. Acta Part A Mol. Biomol. Spectrosc. 227 (2020), 117674, https://doi.org/10.1016/j.saa.2019.117674.

[126] I. Abusallout, G. Hua, Solar photocatalytic degradation of total organic halogen in water using TiO2 catalyst (Dec), Chemosphere 308 (2022), 136206, https://doi.org/10.1016/j.chemosphere.2022.136206.

[127] H. Benkhennouche-Bouchene, et al., Green synthesis of N/Zr Co-doped TiO2 for photocatalytic degradation of p-nitrophenol in wastewater, Catalysts 11 (2) (2021) 1–21, https://doi.org/10.3390/catal11020235.

[128] M. Salimi, et al., A new nano-photocatalyst based on Pt and Bi co-doped TiO2 for efficient visible-light photo degradation of amoxicillin, N. J. Chem. 43 (3) (2019) 1562–1568, https://doi.org/10.1039/c8nj05020a.

[129] C. Yu, J.C. Yu, A simple way to prepare C-N-codoped TiO2 photocatalyst with visible-light activity, Catal. Lett. 129 (3–4) (2009) 462–470, https://doi.org/10.1007/s10562-008-9824-7.

[130] H.R. Pouretedal, Visible photocatalytic activity of co-doped TiO2/Zr,N nanoparticles in wastewater treatment of nitrotoluene samples (Feb), J. Alloy. Compd. 735 (2018) 2507–2511, https://doi.org/10.1016/J.JALLCOM.2017.12.018.

[131] M. Sayed, et al., Narrowing the band gap of TiO2 by co-doping with Mn2+ and Co2+ for efficient photocatalytic degradation of enoxacin and its additional peroxidase like activity: A mechanistic approach (Dec), J. Mol. Liq. 272 (2018) 403–412, https://doi.org/10.1016/J.MOLLIQ.2018.09.102.

[132] L. Munguti, F. Dejene, Influence of annealing temperature on structural, optical and photocatalytic properties of ZnO–TiO2 composites for application in dye removal in water (Oct), Nano-Struct. Nano-Objects 24 (2020), 100594, https://doi.org/10.1016/J.NANOSO.2020.100594.

[133] A. Shahat, K.T. Kubra, M.S. Salman, M.M. Hasan, Novel solid-state sensor material for efficient cadmium(II) detection and capturing from wastewater, Microchem. J. 164 (2021), 105967, https://doi.org/10.1016/j.microc.2021.105967.

[134] V. Vaiano, O. Sacco, D. Sannino, M. Stoller, P. Ciambelli, A. Chianese, Photocatalytic removal of phenol by ferromagnetic N-TiO2/SiO2/Fe3O4 nanoparticles in presence of visible light irradiation, Chem. Eng. Trans. 47 (March) (2016) 235–240, https://doi.org/10.3303/CET1647040.

[135] S. Shukrullah, W. Bashir, N.U.H. Altaf, Y. Khan, A.A. Al-Arainy, T.A. Sheikh, Catalytic and non-catalytic treatment of industrial wastewater under the exposure of non-thermal plasma jet, Processes 8 (6) (2020), https://doi.org/10.3390/PR8060667.

[136] B. Jiang, et al., Review on electrical discharge plasma technology for wastewater remediation, Chem. Eng. J. 236 (2014) 348–368, https://doi.org/10.1016/j.cej.2013.09.090.

[137] M. Russo, G. Iervolino, V. Vaiano, V. Palma, Non-thermal plasma coupled with catalyst for the degradation of water pollutants: A review, Catalysts 10 (12) (2020) 1–29, https://doi.org/10.3390/catal10121438.

[138] H. Wang, J. Li, X. Quan, Y. Wu, Enhanced generation of oxidative species and phenol degradation in a discharge plasma system coupled with TiO2 photocatalysis (Sep), Appl. Catal. B Environ. 83 (1–2) (2008) 72–77, https://doi.org/10.1016/J.APCATB.2008.02.004.

[139] M.S. Salman, M.N. Hasan, K.T. Kubra, M.M. Hasan, Optical detection and recovery of Yb(III) from waste sample using novel sensor ensemble nanomaterials, Microchem. J. 162 (2021), 105868, https://doi.org/10.1016/j.microc.2020.105868.

[140] X.L. Hao, M.H. Zhou, L.C. Lei, Non-thermal plasma-induced photocatalytic degradation of 4-chlorophenol in water (Mar), J. Hazard. Mater. 141 (3) (2007) 475–482, https://doi.org/10.1016/J.JHAZMAT.2006.07.012.

[141] K.T. Kubra, M.S. Salman, H. Znad, M.N. Hasan, Efficient encapsulation of toxic dye from wastewater using biodegradable polymeric adsorbent, J. Mol. Liq. 329 (2021), 115541, https://doi.org/10.1016/j.molliq.2021.115541.

[142] J. Li, Z. Zhou, H. Wang, G. Li, Y. Wu, Research on decoloration of dye wastewater by combination of pulsed discharge plasma and TiO2 nanoparticles, Desalination 212 (1–3) (. 2007) 123–128, https://doi.org/10.1016/J.DESAL.2006.10.006.

[143] K.N. Pandiyaraj, et al., Dye wastewater degradation by the synergetic effect of an atmospheric pressure plasma treatment and the photocatalytic activity of plasma-functionalized Cu–TiO2 nanoparticles, J. Hazard. Mater. 405 (2021), 124264, https://doi.org/10.1016/j.jhazmat.2020.124264.

[144] G.H. Al-Hazmi, M.S. Refat, K.F. Alshammari, K.T. Kubra, A. Shahat, Efficient toxic doxorubicin hydrochloride removal from aqueous solutions using facial alumina nanorods, J. Mol. Struct. 1272 (2023), 134187, https://doi.org/10.1016/j.molstruc.2022.134187.

[145] A. Shahat, K.T. Kubra, A. El-marghany, Equilibrium, thermodynamic and kinetic modeling of triclosan adsorption on mesoporous carbon nanosphere: Optimization using Box-Behnken design, J. Mol. Liq. 383 (2023), 122166, https://doi.org/10.1016/j.molliq.2023.122166.

[146] S. Mustapha, et al., 1, Application of TiO2 and ZnO nanoparticles immobilized on clay in wastewater treatment: a review, 10, Springer International Publishing,, 2020.

[147] M.C. Dlamini, M.S. Maubane-Nkadimeng, J.A. Moma, The use of TiO2/clay heterostructures in the photocatalytic remediation of water containing organic pollutants: A review, J. Environ. Chem. Eng. 9 (6) (2021), 106546, https://doi.org/10.1016/j.jece.2021.106546.

[148] M.C. Sheikh, M.M. Hasan, M.N. Hasan, M.S. Salman, K.T. Kubra, M.E. Awual, R.M. Waliullah, A.I. Rasee, A.I. Rehan, M.S. Hossain, H.M. Marwani, A. Islam, M.A. Khaleque, M.R. Awual, Toxic cadmium(II) monitoring and removal from aqueous solution using ligand-based facial composite adsorbent, J. Mol. Liq. 389 (2023), 122854, https://doi.org/10.1016/j.molliq.2023.122854.

[149] C. Li, et al., A review of clay based photocatalysts: Role of phyllosilicate mineral in interfacial assembly, microstructure control and performance regulation (Jun), Chemosphere 273 (2021) 129723, https://doi.org/10.1016/J.CHEMOSPHERE.2021.129723.

[150] K.G. Bhattacharyya, S. Sen Gupta, Adsorption of a few heavy metals on natural and modified kaolinite and montmorillonite: A review, Adv. Colloid Interface Sci. 140 (2) (2008) 114–131, https://doi.org/10.1016/J.CIS.2007.12.008.

[151] M. Huo, H. Guo, Y. Jiang, H. Ju, B. Xue, F. Li, A facile method of preparing sandwich layered TiO2 in between montmorillonite sheets and its enhanced UV-

light photocatalytic activity, J. Photochem. Photobiol. A Chem. 358 (2018) 121–129, https://doi.org/10.1016/j.jphotochem.2018.02.012.

[152] A.I. Rasee, M.E. Awual, A.I. Rehan, M.S. Hossain, R.M. Waliullah, K.T. Kubra, M.C. Sheikh, M.S. Salman, M.N. Hasan, M.M. Hasan, H.M. Marwani, A. Islam, M.A. Khaleque, M.R. Awual, Efficient separation, adsorption, and recovery of Samarium(III) ions using novel ligand-based composite adsorbent, Surf. Interfaces 41 (2023), 103276, https://doi.org/10.1016/j.surfin.2023.103276.

[153] D. Awfa, M. Ateia, M. Fujii, M.S. Johnson, C. Yoshimura, Photodegradation of pharmaceuticals and personal care products in water treatment using carbonaceous-TiO2 composites: A critical review of recent literature, Water Res 142 (2018) 26–45, https://doi.org/10.1016/j.watres.2018.05.036.

[154] R. Krakowiak, et al., Titanium dioxide-based photocatalysts for degradation of emerging contaminants including pharmaceutical pollutants, Appl. Sci. 11 (18) (2021), https://doi.org/10.3390/app11188674.

[155] J.O. Tijani, U.O. Momoh, R.B. Salau, M.T. Bankole, A.S. Abdulkareem, W.D. Roos, Synthesis and characterization of Ag2O/B2O3/TiO2 ternary nanocomposites for photocatalytic mineralization of local dyeing wastewater under artificial and natural sunlight irradiation, Environ. Sci. Pollut. Res. 26 (19) (2019) 19942–19967, https://doi.org/10.1007/s11356-019-05124-y.

[156] T. Fazal, et al., Integrating adsorption and photocatalysis: A cost effective strategy for textile wastewater treatment using hybrid biochar-TiO2 composite, vol. 390, Elsevier B.V., 2020.

[157] R.M. Waliullah, A.I. Rehan, M.E. Awual, A.I. Rasee, M.C. Sheikh, M.S. Salman, M.S. Hossain, M.M. Hasan, K.T. Kubra, M.N. Hasan, H.M. Marwani, A. Islam, M.M. Rahman, M.A. Khaleque, M.R. Awual, Optimization of toxic dye removal from contaminated water using chitosan-grafted novel nanocomposite adsorbent, J. Mol. Liq. 388 (2023), 122763, https://doi.org/10.1016/j.molliq.2023.122763.

[158] P. Magesan, S. Sanuja, M.J. Umapathy, Novel hybrid chitosan blended MoO3-TiO2 nanocomposite film: Evaluation of its solar light photocatalytic and antibacterial activities, RSC Adv. 5 (53) (2015) 42506–42515, https://doi.org/10.1039/c5ra05692f.

[159] N. Guo, et al., Microscale hierarchical three-dimensional flowerlike TiO2/PANI composite: Synthesis, characterization, and its remarkable photocatalytic activity on organic dyes under UV-light and sunlight irradiation, J. Phys. Chem. C. 118 (32) (2014) 18343–18355, https://doi.org/10.1021/jp5044927.

[160] G. Jayanthi Kalaivani, S.K. Suja, TiO2 (rutile) embedded inulin - A versatile bio-nanocomposite for photocatalytic degradation of methylene blue, Carbohydr. Polym. 143 (2016) 51–60, https://doi.org/10.1016/j.carbpol.2016.01.054.

[161] J. Gomes, J. Lincho, E. Domingues, R. Quinta-Ferreira, R. Martins, N–TiO2 Photocatalysts: A Review of Their Characteristics and Capacity for Emerging Contaminants Removal (Feb), Water 11 (2) (2019) 373, https://doi.org/10.3390/w11020373.

[162] H. Dong, et al., An overview on limitations of TiO2-based particles for photocatalytic degradation of organic pollutants and the corresponding countermeasures (Aug), Water Res 79 (2015) 128–146, https://doi.org/10.1016/j.watres.2015.04.038.

[163] C.-G. Lee, et al., Porous Electrospun Fibers Embedding TiO 2 for Adsorption and Photocatalytic Degradation of Water Pollutants (Apr), Environ. Sci. Technol. 52 (7) (2018) 4285–4293, https://doi.org/10.1021/acs.est.7b06508.

[164] B. Gao, P.S. Yap, T.M. Lim, T.-T. Lim, Adsorption-photocatalytic degradation of Acid Red 88 by supported TiO2: Effect of activated carbon support and aqueous anions (Jul), Chem. Eng. J. 171 (3) (2011) 1098–1107, https://doi.org/10.1016/j.cej.2011.05.006.

[165] P. Cervantes-Avilés, N. Camarillo Piñas, J. Ida, G. Cuevas-Rodríguez, Influence of wastewater type on the impact generated by TiO2 nanoparticles on the oxygen uptake rate in activated sludge process (Apr), J. Environ. Manag. 190 (2017) 35–44, https://doi.org/10.1016/j.jenvman.2016.12.054.

[166] S. Mallakpour, E. Nikkhoo, Surface modification of nano-TiO2 with trimellitylimido-amino acid-based diacids for preventing aggregation of nanoparticles (Jan), Adv. Powder Technol. 25 (1) (2014) 348–353, https://doi.org/10.1016/j.apt.2013.05.017.

[167] E. Kusiak-Nejman, A.W. Morawski, TiO2/graphene-based nanocomposites for water treatment: A brief overview of charge carrier transfer, antimicrobial and photocatalytic performance (Sep), Appl. Catal. B Environ. 253 (2019) 179–186, https://doi.org/10.1016/j.apcatb.2019.04.055.

[168] N. Raza, et al., Solar-light-active silver phosphate/titanium dioxide/silica heterostructures for photocatalytic removal of organic dye (May), J. Clean. Prod. 254 (2020), 120031, https://doi.org/10.1016/j.jclepro.2020.120031.

[169] O. Ola, M.M. Maroto-Valer, Review of material design and reactor engineering on TiO2 photocatalysis for CO2 reduction (Sep), J. Photochem. Photobiol. C. Photochem. Rev. 24 (2015) 16–42, https://doi.org/10.1016/j.jphotochemrev.2015.06.001.

[170] N. Kanth, W. Xu, U. Prasad, D. Ravichandran, A.M. Kannan, K. Song, PMMA-TiO2 Fibers for the Photocatalytic Degradation of Water Pollutants (Jun), Nanomaterials 10 (7) (2020) 1279, https://doi.org/10.3390/nano10071279.

[171] L. Rizzo, D. Sannino, V. Vaiano, O. Sacco, A. Scarpa, D. Pietrogiacomi, Effect of solar simulated N-doped TiO2 photocatalysis on the inactivation and antibiotic resistance of an E. coli strain in biologically treated urban wastewater, Appl. Catal. B Environ. 144 (2014) 369–378, https://doi.org/10.1016/j.apcatb.2013.07.033.

[172] A. Rey, P. García-Muñoz, M.D. Hernández-Alonso, E. Mena, S. García-Rodríguez, F.J. Beltrán, WO3-TiO2 based catalysts for the simulated solar radiation assisted photocatalytic ozonation of emerging contaminants in a municipal wastewater treatment plant effluent, Appl. Catal. B Environ. 154–155 (2014) 274–284, https://doi.org/10.1016/j.apcatb.2014.02.035.

[173] J.J. Rueda-Márquez, C. Palacios-Villarreal, M. Manzano, E. Blanco, M. Ramírez del Solar, I. Levchuk, Photocatalytic degradation of pharmaceutically active compounds (PhACs) in urban wastewater treatment plants effluents under controlled and natural solar irradiation using immobilized TiO2 (August), Sol. Energy 208 (2020) 480–492, https://doi.org/10.1016/j.solener.2020.08.028.

[174] S. Kiran, et al., Photocatalysis using titanium dioxide for treatment of textile wastewater containing disperse dyes, Chiang Mai J. Sci. 45 (7) (2018) 2730–2739.

[175] A.A. Isari, A. Payan, M. Fattahi, S. Jorfi, B. Kakavandi, Photocatalytic degradation of rhodamine B and real textile wastewater using Fe-doped TiO 2 anchored on reduced graphene oxide (Fe-TiO 2 /rGO): Characterization and feasibility, mechanism and pathway studies, Appl. Surf. Sci. 462 (2018) 549–564, https://doi.org/10.1016/j.apsusc.2018.08.133.

[176] B. Neppolian, H.C. Choi, S. Sakthivel, B. Arabindoo, V. Murugesan, Solar light induced and TiO2 assisted degradation of textile dye reactive blue 4, Chemosphere 46 (8) (2002) 1173–1181, https://doi.org/10.1016/S0045-6535(01)00284-3.

[177] A.Y. Zhang, W.K. Wang, D.N. Pei, H.Q. Yu, Degradation of refractory pollutants under solar light irradiation by a robust and self-protected ZnO/CdS/TiO2 hybrid photocatalyst, Water Res 92 (2016) 78–86, https://doi.org/10.1016/j.watres.2016.01.045.

[178] M. Tanveer, G.T. Guyer, G. Abbas, Photocatalytic degradation of ibuprofen in water using TiO2 and ZnO under artificial UV and solar irradiation, Water Environ. Res. 91 (9) (2019) 822–829, https://doi.org/10.1002/wer.1104.

[179] Y. He, N.B. Sutton, H.H.H. Rijnaarts, A.A.M. Langenhoff, Degradation of pharmaceuticals in wastewater using immobilized TiO2 photocatalysis under simulated solar irradiation, Appl. Catal. B Environ. 182 (2016) 132–141, https://doi.org/10.1016/j.apcatb.2015.09.015.

[180] M. Gar Alalm, A. Tawfik, S. Ookawara, Enhancement of photocatalytic activity of TiO2 by immobilization on activated carbon for degradation of pharmaceuticals, J. Environ. Chem. Eng. 4 (2) (2016) 1929–1937, https://doi.org/10.1016/j.jece.2016.03.023.

[181] J.O. Haolat, A. George, M. Issa Suleiman, M. Berthod, K. Wang, UV-TiO2 treatment of the cooling water of an oil refinery (October), J. Water Process Eng. 26 (2018) 176–181, https://doi.org/10.1016/j.jwpe.2018.10.013.

[182] W.Z. Khan, I. Najeeb, M. Tuiyebayeva, Z. Makhteyeva, Refinery wastewater degradation with Titanium dioxide, Zinc oxide, and Hydrogen peroxide in a photocatalytic reactor, Soc. Pet. Eng. - 1st SPE Afr. Heal. Saf., Secur. Environ. Soc. Responsib. Conf. Exhib. 2014 - Prot. People Environ. Get. it Right Dev. Oil Gas. Ind. (2014) 215–225, https://doi.org/10.2118/170221-ms.

[183] A. García-Ripoll, A. Arques, R. Vicente, A. Domenech, A.M. Amat, Treatment of aqueous solutions containing four commercial pesticides by means of TiO2 solar photocatalysis, J. Sol. Energy Eng. Trans. ASME 130 (4) (2008) 0410111–0410115, https://doi.org/10.1115/1.2969810.

[184] A.M. Amat, A. Arques, F. López, M.A. Miranda, Solar photo-catalysis to remove paper mill wastewater pollutants, Sol. Energy 79 (4) (2005) 393–401, https://doi.org/10.1016/j.solener.2005.02.021.

[185] M.Y. Ghaly, T.S. Jamil, I.E. El-Seesy, E.R. Souaya, R.A. Nasr, Treatment of highly polluted paper mill wastewater by solar photocatalytic oxidation with synthesized nano TiO2, Chem. Eng. J. 168 (1) (2011) 446–454, https://doi.org/10.1016/j.cej.2011.01.028.

[186] P. Sun, et al., Photocatalyst of organic pollutants decomposition: TiO2/glass fiber cloth composites, Catal. Today 274 (2016) 2–7, https://doi.org/10.1016/j.cattod.2016.04.036.

[187] N. Vela, et al., Solar reclamation of wastewater effluent polluted with bisphenols, phthalates and parabens by photocatalytic treatment with TiO2/Na2S2O8 at pilot plant scale, Chemosphere 212 (2018) 95–104, https://doi.org/10.1016/j.chemosphere.2018.08.069.

[188] P. Al, İ.C. Ğ. Lu, D.T. Sponza, EFFECT OF GRAPHENE-TiO 2 ON THE PHOTODEGRADATION OF OLIVE MILL EFFLUENT AND RECOVERY OF GRAPHENE-TiO 2, Sigma J. Eng. Nat. Sci. 8 (3) (2017) 227–234.

[189] S. Adish Kumar, G.S. Sree Lekshmi, J. Rajesh Banu, I. Tae Yeom, Synergistic degradation of hospital wastewater by solar/ TiO2/Fe2+ /H2O2 process, Water Qual. Res. J. Can. 49 (3) (2014) 223–233, https://doi.org/10.2166/wqrjc.2014.026.

[190] T. Keijer, V. Bakker, J.C. Slootweg, Circular chemistry to enable a circular economy (Mar), Nat. Chem. 11 (3) (2019) 190–195, https://doi.org/10.1038/s41557-019-0226-9.

[191] S.A. Rawool, et al., pn Heterojunctions in NiO:TiO2 composites with type-II band alignment assisting sunlight driven photocatalytic H2 generation (Feb), Appl. Catal. B Environ. 221 (2018) 443–458, https://doi.org/10.1016/j.apcatb.2017.09.004.

[192] M. Argyle, C. Bartholomew, Heterogeneous Catalyst Deactivation and Regeneration: A Review (Feb), Catalysts 5 (1) (2015) 145–269, https://doi.org/10.3390/catal5010145.

[193] S. Salaeh, et al., Reuse of TiO 2 -based catalyst for solar driven water treatment; thermal and chemical reactivation (Jan), J. Photochem. Photobiol. A Chem. 333 (2017) 117–129, https://doi.org/10.1016/j.jphotochem.2016.10.015.

[194] E.M. Saggioro, A.S. Oliveira, T. Pavesi, C.G. Maia, L.F.V. Ferreira, J.C. Moreira, Use of Titanium Dioxide Photocatalysis on the Remediation of Model Textile Wastewaters Containing Azo Dyes (Dec), Molecules 16 (12) (2011) 10370–10386, https://doi.org/10.3390/molecules161210370.

[195] N. Miranda-García, S. Suárez, M.I. Maldonado, S. Malato, B. Sánchez, Regeneration approaches for TiO2 immobilized photocatalyst used in the elimination of emerging contaminants in water (Jul), Catal. Today 230 (2014) 27–34, https://doi.org/10.1016/j.cattod.2013.12.048.

[196] V.G. Gandhi, M.K. Mishra, P.A. Joshi, A study on deactivation and regeneration of titanium dioxide during photocatalytic degradation of phthalic acid (Nov), J. Ind. Eng. Chem. 18 (6) (2012) 1902–1907, https://doi.org/10.1016/j.jiec.2012.05.001.

[197] A. Fallah Shojaei, A. Shams-Nateri, M. Ghomashpasand, Comparative study of photocatalytic activities of magnetically separable WO3/TiO2/Fe3O4 nanocomposites and TiO2, WO3/TiO2 and TiO2/Fe3O4 under visible light irradiation, Superlattices Microstruct. 88 (2015) 211–224, https://doi.org/10.1016/j.spmi.2015.09.014.

[198] W. Ahmad, et al., Photocatalytic degradation of crystal violet dye under sunlight by chitosan-encapsulated ternary metal selenide microspheres (Feb), Environ. Sci. Pollut. Res. 28 (7) (2021) 8074–8087, https://doi.org/10.1007/s11356-020-10898-7.

[199] K. Sonu, S.H. Puttaiah, V.S. Raghavan, S.S. Gorthi, Photocatalytic degradation of MB by TiO2: studies on recycle and reuse of photocatalyst and treated water for seed germination (Sep), Environ. Sci. Pollut. Res. 28 (35) (2021) 48742–48753, https://doi.org/10.1007/s11356-021-13863-0.

[200] S. Alberti, V. Caratto, D. Peddis, C. Belviso, M. Ferretti, Synthesis and characterization of a new photocatalyst based on TiO2 nanoparticles supported on a magnetic zeolite obtained from iron and steel industrial waste (Aug), J. Alloy. Compd. 797 (2019) 820–825, https://doi.org/10.1016/j.jallcom.2019.05.098.

[201] M. Kumar, S. Ambika, A. Hassani, P.V. Nidheesh, Waste to catalyst: Role of agricultural waste in water and wastewater treatment (Feb), Sci. Total Environ. 858 (2023), 159762, https://doi.org/10.1016/j.scitotenv.2022.159762.

[202] I. Thakur, A. Verma, B. Örmeci, Inactivation of bacteria present in secondary municipal wastewater effluent using the hybrid effect of Fe–TiO2 catalyst (Jun), J. Clean. Prod. 352 (2022), 131575, https://doi.org/10.1016/j.jclepro.2022.131575.

[203] Y.K. Dasan, M.K. Lam, S. Yusup, J.W. Lim, K.T. Lee, Life cycle evaluation of microalgae biofuels production: Effect of cultivation system on energy, carbon emission and cost balance analysis (Oct), Sci. Total Environ. 688 (2019) 112–128, https://doi.org/10.1016/j.scitotenv.2019.06.181.

[204] J. Giménez, B. Bayarri, Ó. González, S. Malato, J. Peral, S. Esplugas, Advanced oxidation processes at laboratory scale: environmental and economic impacts (Dec), ACS Sustain. Chem. Eng. 3 (12) (2015) 3188–3196, https://doi.org/10.1021/acssuschemeng.5b00778.

[205] J. Musial, D.T. Mlynarczyk, B.J. Stanisz, Photocatalytic degradation of sulfamethoxazole using TiO2-based materials – Perspectives for the development of a sustainable water treatment technology (Jan), Sci. Total Environ. 856 (2023), 159122, https://doi.org/10.1016/j.scitotenv.2022.159122.

[206] K.F. Shariar, E.G. Ovy, and T.A. Hossainy, "Closed Environment Design of Solar Collector Trough using Lenses and Reflectors," Nov. 2011, pp. 3852–3858, doi: 10.3384/ecp110573852.

[207] R.C. Asha, M.A. Vishnuganth, N. Remya, N. Selvaraju, M. Kumar, Livestock wastewater treatment in batch and continuous photocatalytic systems: performance and economic analyses, Water, Air, Soil Pollut. 226 (5) (2015) 132, https://doi.org/10.1007/s11270-015-2396-4.

[208] A. Balakrishnan, K. Gopalram, S. Appunni, Photocatalytic degradation of 2,4-dicholorophenoxyacetic acid by TiO2 modified catalyst: kinetics and operating cost analysis, Environ. Sci. Pollut. Res. 28 (25) (2021) 33331–33343, https://doi.org/10.1007/s11356-021-12928-4.

[209] A. Asadi, R. Akbarzadeh, A. Eslami, T.-C. Jen, and P. Ozaveshe Oviroh, "Effect of synthesis method on NS-TiO2 photocatalytic performance," *Energy Procedia*, 158, pp. 4542–4547, Feb. 2019, doi: 10.1016/j.egypro.2019.01.756.

[210] M. Gar Alalm, A. Tawfik, S. Ookawara, Comparison of solar TiO2 photocatalysis and solar photo-Fenton for treatment of pesticides industry wastewater: Operational conditions, kinetics, and costs, J. Water Process Eng. 8 (2015) 55–63, https://doi.org/10.1016/j.jwpe.2015.09.007.

[211] B. Prasai, B. Cai, M.K. Underwood, J.P. Lewis, D.A. Drabold, Properties of amorphous and crystalline titanium dioxide from first principles (Nov), J. Mater. Sci. 47 (21) (2012) 7515–7521, https://doi.org/10.1007/s10853-012-6439-6.

[212] C.E. Ekuma, D. Bagayoko, Ab-initio electronic and structural properties of rutile titanium dioxide (Oct), Jpn. J. Appl. Phys. 50 (10) (2011), 101103, https://doi.org/10.1143/JJAP.50.101103.

[213] T. Arlt, et al., High-pressure polymorphs of anatase (Jun), Phys. Rev. B 61 (21) (2000) 14414–14419, https://doi.org/10.1103/PhysRevB.61.14414.

[214] M. Mohamad, B.U. Haq, R. Ahmed, A. Shaari, N. Ali, R. Hussain, A density functional study of structural, electronic and optical properties of titanium dioxide: characterization of rutile, anatase and brookite polymorphs (Mar), Mater. Sci. Semicond. Process. 31 (2015) 405–414, https://doi.org/10.1016/j.mssp.2014.12.027.

[215] P.V. Bakre, P.S. Volvoikar, A.A. Vernekar, S.G. Tilve, Influence of acid chain length on the properties of TiO2 prepared by sol-gel method and LC-MS studies of methylene blue photodegradation, J. Colloid Interface Sci. 474 (2016) 58–67, https://doi.org/10.1016/j.jcis.2016.04.011.

[216] K. Wetchakun, N. Wetchakun, S. Sakulsermsuk, An overview of solar/visible light-driven heterogeneous photocatalysis for water purification: TiO2- and ZnO-based photocatalysts used in suspension photoreactors, J. Ind. Eng. Chem. 71 (2019) 19–49, https://doi.org/10.1016/j.jiec.2018.11.025.

[217] F. Azeez, et al., The effect of surface charge on photocatalytic degradation of methylene blue dye using chargeable titania nanoparticles, Sci. Rep. 8 (1) (2018) 1–9, https://doi.org/10.1038/s41598-018-25673-5.

[218] D. Mardare, et al., Synthesis and hydrophilic properties of Mo doped TiO2 thin films, J. Appl. Phys. 115 (21) (2014), 213501, https://doi.org/10.1063/1.4880339.

[219] M. Ji, Y.H. Choa, Y.I. Lee, One-step synthesis of black TiO2-x microspheres by ultrasonic spray pyrolysis process and their visible-light-driven photocatalytic activities, Ultrason. Sonochem. 74 (2021), 105557, https://doi.org/10.1016/j.ultsonch.2021.105557.

[220] N. Kanjana, W. Maiaugree, P. Poolcharuansin, P. Laokul, Size controllable synthesis and photocatalytic performance of mesoporous TiO2 hollow spheres, J. Mater. Sci. Technol. 48 (2020) 105–113, https://doi.org/10.1016/j.jmst.2020.03.013.

[221] J. Prakash, et al., Novel rare earth metal–doped one-dimensional TiO2 nanostructures: Fundamentals and multifunctional applications, Mater. Today Sustain. 13 (2021), 100066, https://doi.org/10.1016/j.mtsust.2021.100066.

[222] M. Bordbar, T. Alimohammadi, B. Khoshnevisan, B. Khodadadi, A. Yeganeh-Faal, Preparation of MWCNT/TiO2-Co nanocomposite electrode by electrophoretic deposition and electrochemical study of hydrogen storage, Int. J. Hydrog. Energy 40 (31) (2015) 9613–9620, https://doi.org/10.1016/j.ijhydene.2015.05.138.

[223] X. Liu, et al., Synergistic degradation of acid orange 7 dye by using non-thermal plasma and g-C3N4/TiO2: Performance, degradation pathways and catalytic mechanism (Jun), Chemosphere 249 (2020), 126093, https://doi.org/10.1016/J.CHEMOSPHERE.2020.126093.

[224] O.K. Mmelesi, N. Masunga, A. Kuvarega, T.T. Nkambule, B.B. Mamba, K.K. Kefeni, Cobalt ferrite nanoparticles and nanocomposites: Photocatalytic, antimicrobial activity and toxicity in water treatment (April), Mater. Sci. Semicond. Process. 123 (2021), 105523, https://doi.org/10.1016/j.mssp.2020.105523.

[225] K. Kądzioła, I. Piwoński, A. Kisielewska, D. Szczukocki, B. Krawczyk, J. Sielski, The photoactivity of titanium dioxide coatings with silver nanoparticles prepared by sol-gel and reactive magnetron sputtering methods - Comparative studies, Appl. Surf. Sci. 288 (2014) 503–512, https://doi.org/10.1016/j.apsusc.2013.10.061.

[226] Z. Wang, et al., Preparation and characterization of TiO2 nanoparticles by two different precipitation methods, Ceram. Int. 46 (10) (2020) 15333–15341, https://doi.org/10.1016/j.ceramint.2020.03.075.

[227] M. Malekshahi Byranvand, A. Nemati Kharat, L. Fatholahi, Z. Malekshahi Beiranvand, A review on synthesis of nano-TiO2 via different methods, J. Nanostruct. 3 (1) (2013) 1–9, https://doi.org/10.7508/jns.2013.01.001.

[228] C.M. Magdalane, G.M.A. Priyadharsini, K. Kaviyarasu, A.I. Jothi, G.G. Simiyon, Synthesis and characterization of TiO2 doped cobalt ferrite nanoparticles via microwave method: Investigation of photocatalytic performance of congo red degradation dye, August 2020, Surf. Interfaces 25 (2021), 101296, https://doi.org/10.1016/j.surfin.2021.101296.

[229] A.D. Terna, E.E. Elemike, J.I. Mbonu, O.E. Osafile, R.O. Ezeani, The future of semiconductors nanoparticles: Synthesis, properties and applications, December 2020, Mater. Sci. Eng. B Solid-State Mater. Adv. Technol. 272 (2021), 115363, https://doi.org/10.1016/j.mseb.2021.115363.

[230] J. Lv, et al., Enhanced visible light photocatalytic activity of TiO2 nanotube arrays modified with CdSe nanoparticles by electrodeposition method, Surf. Coat. Technol. 242 (2014) 20–28, https://doi.org/10.1016/j.surfcoat.2014.01.006.

[231] J.H. Lee, T. Kim, E.R. Kim, E.B. Cho, S.C. Jung, Microwave-assisted synthesis of various Cu2O/Cu/TiO2 and CuxS/TiO2 composite nanoparticles towards visible-light photocatalytic applications, November 2020, Mater. Chem. Phys. 259 (2021), 123986, https://doi.org/10.1016/j.matchemphys.2020.123986.

[232] V.M. Ramakrishnan, M. Natarajan, A. Santhanam, V. Asokan, D. Velauthapillai, Size controlled synthesis of TiO2 nanoparticles by modified solvothermal method towards effective photo catalytic and photovoltaic applications, Mater. Res. Bull. 97 (2018) 351–360, https://doi.org/10.1016/j.materresbull.2017.09.017.

[233] V.D. Potle, S.R. Shirsath, B.A. Bhanvase, V.K. Saharan, Sonochemical preparation of ternary rGO-ZnO-TiO2 nanocomposite photocatalyst for efficient degradation of crystal violet dye, Optics 208 (March) (2020), 164555, https://doi.org/10.1016/j.ijleo.2020.164555.

[234] R. Nainani, P. Thakur, M. Chaskar, Synthesis of silver doped TiO 2 nanoparticles for the improved photocatalytic degradation of methyl orange, J. Mater. Sci. Eng. B 2 (1) (2012) 52–58.

[235] L. Huang, et al., Facile and large-scale preparation of N doped TiO2 photocatalyst with high visible light photocatalytic activity (Dec), Mater. Lett. 209 (2017) 585–588, https://doi.org/10.1016/J.MATLET.2017.08.092.

[236] T.H. Kim, G.M. Go, H.B. Cho, Y. Song, C.G. Lee, Y.H. Choa, A novel synthetic method for N Doped TiO2 nanoparticles through plasma-assisted electrolysis and photocatalytic activity in the visible region, Front. Chem. 6 (SEP) (2018) 1–10, https://doi.org/10.3389/fchem.2018.00458.

[237] S.A. Bakar, C. Ribeiro, A comparative run for visible-light-driven photocatalytic activity of anionic and cationic S-doped TiO2 photocatalysts: a case study of possible sulfur doping through chemical protocol, J. Mol. Catal. A Chem. 421 (2016) 1–15, https://doi.org/10.1016/J.MOLCATA.2016.05.003.

[238] F. Wang, et al., S-TiO2 with enhanced visible-light photocatalytic activity derived from TiS2 in deionized water (Mar), Mater. Res. Bull. 87 (2017) 20–26, https://doi.org/10.1016/J.MATERRESBULL.2016.11.014.

[239] M.R.D. Khaki, B. Sajjadi, A.A.A. Raman, W.M.A.W. Daud, S. Shmshirband, Sensitivity analysis of the photoactivity of Cu-TiO2/ZnO during advanced oxidation reaction by Adaptive Neuro-Fuzzy Selection Technique, Meas. J. Int. Meas. Confed. 77 (2016) 155–174, https://doi.org/10.1016/j.measurement.2015.07.004.

[240] C. Lu, et al., Preparation of Er3+:YAlO3/Fe- and Co-doped TiO2–ZnO coated composites and their visible-light photocatalytic activity in degradation of some organic dyes, Res. Chem. Intermed. 42 (5) (2016) 4651–4668, https://doi.org/10.1007/s11164-015-2306-9.

[241] Y. Lu, M. Yao, A. Zhou, Q. Hu, L. Wang, Preparation and photocatalytic performance of Ti3C2/TiO2/CuO ternary nanocomposites, J. Nanomater. 2017 (2017) 1–6, https://doi.org/10.1155/2017/1978764.

[242] R.G. Ciocarlan, et al., Novel magnetic nanocomposites containing quaternary ferrites systems Co0.5Zn0.25M0.25Fe2O4 (M = Ni, Cu, Mn, Mg) and TiO2-anatase phase as photocatalysts for wastewater remediation under solar light irradiation, December 2017, Mater. Sci. Eng. B Solid-State Mater. Adv. Technol. 230 (2018) 1–7, https://doi.org/10.1016/j.mseb.2017.12.030.

[243] J. Saien, Z. Mesgari, Photocatalytic degradation of methyl orange using hematoporphyrin/N-doped TiO2 nanohybrids under visible light: kinetics and energy consumption, Appl. Organomet. Chem. 31 (11) (2017) 1–11, https://doi.org/10.1002/aoc.3755.

[244] X. Yan, et al., The interplay of sulfur doping and surface hydroxyl in band gap engineering: mesoporous sulfur-doped TiO2 coupled with magnetite as a recyclable, efficient, visible light active photocatalyst for water purification (Dec), Appl. Catal. B Environ. 218 (2017) 20–31, https://doi.org/10.1016/J.APCATB.2017.06.022.

[245] M.N. Chong, Z.Y. Tneu, P.E. Poh, B. Jin, R. Aryal, Synthesis, characterisation and application of TiO2–zeolite nanocomposites for the advanced treatment of industrial dye wastewater (May), J. Taiwan Inst. Chem. Eng. 50 (2015) 288–296, https://doi.org/10.1016/J.JTICE.2014.12.013.

[246] F. Maraschi, et al., TiO2-modified zeolites for fluoroquinolones removal from wastewaters and reuse after solar light regeneration (Dec), J. Environ. Chem. Eng. 2 (4) (2014) 2170–2176, https://doi.org/10.1016/J.JECE.2014.08.009.

[247] Y. Li, et al., Enhanced photocatalytic degradation of organic dyes via defect-rich tio2 prepared by dielectric barrier discharge plasma, Nanomaterials 9 (5) (2019), https://doi.org/10.3390/nano9050720.

[248] H. Guo, et al., Enhanced catalytic performance of graphene-TiO2 nanocomposites for synergetic degradation of fluoroquinolone antibiotic in pulsed discharge plasma system, October 2018, Appl. Catal. B Environ. 248 (2019) 552–566, https://doi.org/10.1016/j.apcatb.2019.01.052.

[249] A. Hafeez, N. Shezad, F. Javed, T. Fazal, M. Saif ur Rehman, F. Rehman, Synergetic effect of packed-bed corona-DBD plasma micro-reactor and photocatalysis for organic pollutant degradation (Aug), Sep. Purif. Technol. 269 (2021), 118728, https://doi.org/10.1016/J.SEPPUR.2021.118728.

[250] T. Mitrović, N. Tomić, A. Djukić-Vuković, Z. Dohčević-Mitrović, S. Lazović, Atmospheric Plasma Supported by TiO2 Catalyst for Decolourisation of Reactive Orange 16 Dye in Water, Waste Biomass-.-. Valoriz. 11 (12) (2020) 6841–6854, https://doi.org/10.1007/s12649-019-00928-y.

[251] J. Wang, Y. Sun, J. Feng, L. Xin, J. Ma, Degradation of triclocarban in water by dielectric barrier discharge plasma combined with TiO2/activated carbon fibers: Effect of operating parameters and byproducts identification (Sep), Chem. Eng. J. 300 (2016) 36–46, https://doi.org/10.1016/J.CEJ.2016.04.041.

[252] G. Zhang, Y. Sun, C. Zhang, Z. Yu, Decomposition of acetaminophen in water by a gas phase dielectric barrier discharge plasma combined with TiO2-rGO nanocomposite: Mechanism and degradation pathway, J. Hazard. Mater. 323 (2017) 719–729, https://doi.org/10.1016/j.jhazmat.2016.10.008.

[253] E. Ahmadi, et al., Synergistic effects of α-Fe2O3-TiO2 and Na2S2O8 on the performance of a non-thermal plasma reactor as a novel catalytic oxidation process for dimethyl phthalate degradation (Nov), Sep. Purif. Technol. 250 (2020), 117185, https://doi.org/10.1016/J.SEPPUR.2020.117185.

[254] Y. Shen, et al., Optimizing degradation of Reactive Yellow 176 by dielectric barrier discharge plasma combined with TiO2 nano-particles prepared using response surface methodology (Mar), J. Taiwan Inst. Chem. Eng. 60 (2016) 302–312, https://doi.org/10.1016/J.JTICE.2015.10.018.

[255] J. Wang, et al., Sonocatalytic degradation of organic dyes and comparison of catalytic activities of CeO2/TiO2, SnO2/TiO2 and ZrO2/TiO2 composites under ultrasonic irradiation, Ultrason. Sonochem. 17 (4) (2010) 642–648, https://doi.org/10.1016/j.ultsonch.2009.12.016.

[256] Y. Zhang, R. Zhang, W. Ma, X. Zhang, L. Wang, Z. Guan, Purification of water by bipolar pulsed discharge plasma combined with TiO2 catalysis, J. Phys. Conf. Ser. 418 (1) (2013), https://doi.org/10.1088/1742-6596/418/1/012125.

[257] M. Pinna, et al., Biochar nanoparticles over tio2 nanotube arrays: A green co-catalyst to boost the photocatalytic degradation of organic pollutants, Catalysts 11 (9) (2021), https://doi.org/10.3390/catal11091048.

[258] X. Cai, et al., Titanium dioxide-coated biochar composites as adsorptive and photocatalytic degradation materials for the removal of aqueous organic pollutants, J. Chem. Technol. Biotechnol. 93 (3) (2018) 783–791, https://doi.org/10.1002/jctb.5428.

[259] C.P. Silva, et al., Biochar-TiO2 magnetic nanocomposites for photocatalytic solar-driven removal of antibiotics from aquaculture effluents (May), J. Environ. Manag. 294 (2021), https://doi.org/10.1016/j.jenvman.2021.112937.

[260] M. Bahal, N. Kaur, N. Sharotri, D. Sud, Investigations on amphoteric chitosan/TiO2 bionanocomposites for application in visible light induced photocatalytic degradation, Adv. Polym. Technol. 2019 (2019), https://doi.org/10.1155/2019/2345631.

[261] O.A. Oyewo, N.G. Nevondo, D.C. Onwudiwe, M.S. Onyango, Photocatalytic degradation of methyl blue in water using sawdust-derived cellulose nanocrystals-metal oxide nanocomposite, J. Inorg. Organomet. Polym. Mater. 31 (6) (2021) 2542–2552, https://doi.org/10.1007/s10904-020-01847-5.

[262] G.D. Tarigh, F. Shemirani, N.S. Maz`hari, Fabrication of a reusable magnetic multi-walled carbon nanotube-TiO2 nanocomposite by electrostatic adsorption: Enhanced photodegradation of malachite green, RSC Adv. 5 (44) (2015) 35070–35079, https://doi.org/10.1039/c4ra15593a.

[263] C. Ling, C. Yue, R. Yuan, J. Qiu, F.Q. Liu, J.J. Zhu, Enhanced removal of sulfamethoxazole by a novel composite of TiO2 nanocrystals in situ wrapped-Bi2O4 microrods under simulated solar irradiation (October), Chem. Eng. J. 384 (2020), 123278, https://doi.org/10.1016/j.cej.2019.123278.

[264] S. Xu, G. Xiao, Z. Wang, Y. Wang, Z. Liu, H. Su, A reusable chitosan/TiO2@g-C3N4 nanocomposite membrane for photocatalytic removal of multiple toxic water pollutants under visible light, Water Sci. Technol. 83 (12) (2021) 3063–3074, https://doi.org/10.2166/wst.2021.188.

[265] A. Tripathi, S. Narayanan, Impact of TiO2 and TiO2/g-C3N4 Nanocomposite to Treat Industrial Wastewater, Environ. Nanotechnol., Monit. Manag. 10 (2018) 280–291, https://doi.org/10.1016/j.enmm.2018.07.010.

[266] A.A. Essawy, S.M. Sayyah, A.M. El-Nggar, Wastewater remediation by TiO2-impregnated chitosan nano-grafts exhibited dual functionality: High adsorptivity and solar-assisted self-cleaning, J. Photochem. Photobiol. B Biol. 173 (June) (2017) 170–180, https://doi.org/10.1016/j.jphotobiol.2017.05.044.

[267] H. Asadzadeh Patehkhor, M. Fattahi, M. Khosravi-Nikou, Synthesis and characterization of ternary chitosan–TiO2–ZnO over graphene for photocatalytic degradation of tetracycline from pharmaceutical wastewater, Sci. Rep. 11 (1) (2021) 1–17, https://doi.org/10.1038/s41598-021-03492-5.

[268] T. Lavanya, K. Satheesh, M. Dutta, N. Victor Jaya, N. Fukata, Superior photocatalytic performance of reduced graphene oxide wrapped electrospun anatase mesoporous TiO2 nanofibers, J. Alloy. Compd. 615 (2014) 643–650, https://doi.org/10.1016/j.jallcom.2014.05.088.

[269] R. Atchudan, T.N. Jebakumar Immanuel Edison, S. Perumal, D. Karthikeyan, Y. R. Lee, Effective photocatalytic degradation of anthropogenic dyes using graphene oxide grafting titanium dioxide nanoparticles under UV-light irradiation, J. Photochem. Photobiol. A Chem. 333 (2017) 92–104, https://doi.org/10.1016/j.jphotochem.2016.10.021.

[270] B.K. Gupta, G. Kedawat, Y. Agrawal, P. Kumar, J. Dwivedi, S.K. Dhawan, A novel strategy to enhance ultraviolet light driven photocatalysis from graphene quantum dots infilled TiO2 nanotube arrays, RSC Adv. 5 (14) (2015) 10623–10631, https://doi.org/10.1039/c4ra14039g.

[271] L. Liu, H. Bai, J. Liu, D.D. Sun, Multifunctional graphene oxide-TiO2-Ag nanocomposites for high performance water disinfection and decontamination under solar irradiation, J. Hazard. Mater. 261 (2013) 214–223, https://doi.org/10.1016/j.jhazmat.2013.07.034.

[272] M. Gar Alalm, A. Tawfik, S. Ookawara, Enhancement of photocatalytic activity of TiO2 by immobilization on activated carbon for degradation of pharmaceuticals (Jun), J. Environ. Chem. Eng. 4 (2) (2016) 1929–1937, https://doi.org/10.1016/j.jece.2016.03.023.

[273] M. Jiménez, et al., Supported TiO2 solar photocatalysis at semi-pilot scale: Degradation of pesticides found in citrus processing industry wastewater, reactivity and influence of photogenerated species, J. Chem. Technol. Biotechnol. 90 (1) (2015) 149–157, https://doi.org/10.1002/jctb.4299.

[274] S. Malato, J. Blanco, J. Cáceres, A.R. Fernández-Alba, A. Agüera, A. Rodríguez, Photocatalytic treatment of water-soluble pesticides by photo-Fenton and TiO2 using solar energy, Catal. Today 76 (2–4) (2002) 209–220, https://doi.org/10.1016/S0920-5861(02)00220-1.

[275] M. Uğurlu, M.H. Karaoğlu, Photocatalytic removal of olive mill waste water by TiO2 loaded on sepiolite and under natural solar irradiation (Oct), Environ. Prog. Sustain. Energy 30 (3) (2011) 326–336, https://doi.org/10.1002/ep.10483.

[276] S.G. Poulopoulos, A. Yerkinova, G. Ulykbanova, V.J. Inglezakis, Photocatalytic treatment of organic pollutants in a synthetic wastewater using UV light and combinations of TiO2, H2O2 and Fe(III), PLoS One 14 (5) (2019) 1–20, https://doi.org/10.1371/journal.pone.0216745.

[277] H. Koohestani, Photocatalytic removal of cyanide and Cr(IV) from wastewater in the presence of each other by using TiO 2 /UV, Micro Nano Lett. 14 (1) (2019) 45–50, https://doi.org/10.1049/mnl.2018.5170.

[278] L. Yanyan, T.A. Kurniawan, Z. Ying, A.B. Albadarin, G. Walker, Enhanced photocatalytic degradation of acetaminophen from wastewater using WO3/TiO2/SiO2 composite under UV–VIS irradiation, J. Mol. Liq. 243 (2017) 761–770, https://doi.org/10.1016/j.molliq.2017.08.092.

[279] Y. Zhang, W. Lin, Y. Li, K. Ding, J. Li, A theoretical study on the electronic structures of TiO 2: effect of Hartree−Fock exchange, J. Phys. Chem. B 109 (41) (2005) 19270–19277, https://doi.org/10.1021/jp0523625.